RSC Advances

ROYAL SOCIETY OF CHEMISTRY

www.rsc.org/advances

Synthesis and Sensing Applications of Polyaniline Nanocomposites: A Review

Tanushree Sen, Navinchandra G. Shimpi, Satyendra Mishra*
University Institute of Chemical Technology, North Maharashtra University, Jalgaon - 425001, Maharashtra, India.

A comprehensive review on synthesis of PANI nanocomposites and their applications as gas sensors and biosensors has been presented. The multi-functionality of PANI nanocomposites have been extensively exploited in diverse applications with impressive results. The synergistic effects between the constituents have made these materials particularly attractive as sensing elements for gases and biological agents. Not only do PANI nanocomposites allow room temperature sensing of a large number of combustible or toxic gases and pollutants with high selectivity and sensitivity, they also enable immobilization of bioreceptors such as enzymes, antigen-antibodies, and nucleic acids onto their surfaces for detection of an array of biological agents through a combination of biochemical and electrochemical reactions. Efforts are on towards understanding the working mechanism of PANI nanocomposites which will increase their potential fields of applications.

Keywords: Polyaniline; Nanocomposite; Gas sensor; Biosensors.

---

*Corresponding author: Prof. Satyendra Mishra (profsm@rediffmail.com)
Address: University Institute of Chemical Technology, North Maharashtra University
Jalgaon - 425001, Maharashtra, India
Phone No: +91-257-2258420
Fax No: +91-257-2258403

1. Introduction

Synthetic polymers, since the time of its industrialization, have been popular as electrically insulating materials for over a century. The discovery of electrically conducting polymers, therefore, heralded a new era in the domain of polymer science. The interest of the scientific community in the electrical conductivity in synthetic polymers found its impetus from the pioneering work of Shirakawa, MacDiarmid and Heeger in the field of conducting polymers, for which they received Nobel Prize in Chemistry in 2000. Since then, the field of conducting polymers has gathered momentum owing to the extensive fundamental research carried out in this arena of science, which today includes a host of conjugated polymers such as polyacetylene (PA), polyaniline (PANI), polypyrrole (PPY), poly (p-phenylene) (PPP), poly (p-phenylenevinylene) (PPV), polythiophenes (PTH) and their derivatives [1,2]. These polymers have a backbone of π-conjugated chain, a sequence of alternating single and double bonds (sp^2 hybridized structure), which results in delocalization of π-electrons along the entire polymer chain, consequently lending these polymers their special electrical properties [3,4]. Due to the inherent ability of these polymers to conduct electricity through charge delocalization they are called intrinsically conducting polymers (ICPs). Figure 1 shows molecular structures of some of the prominent conjugated polymers.

Amongst all the ICPs, PANI has been the subject of enormous interest to researchers due to its reversible doping/dedoping character, modifiable electrical conductivity, pH switching properties and good environmental stability [5]. It also possesses the unique ability to get doped by protonic acids (proton doping) apart from the conventional redox doping. Through the virtue of its molecular self-assembly, PANI often forms supramolecular nanofibers, thereby lending itself to a variety of applications due to the radically different and new properties resulting from the high surface to volume ratio. Several nanostructures of PANI such as nanofibers, nanotubes and nanospheres have been prepared by an array of synthesis

methods [6-9]. Introduction of a secondary component, such as nanomaterials, into PANI further extends its functionality, offering efficient designs and enhanced performance. It has been experimentally shown that the synergy between the individual components lend the nanocomposite enhanced characteristics, thereby expanding its scope of application [4,10-12]. The development of PANI nanostructures and their nanocomposites stems from the desire to explore the full potential of these materials.

The secondary component in a nanocomposite can be metallic or bimetallic nanoparticles, metal oxide nanoparticles, carbon compounds such as CNT or graphene, chalcogenides, polymers, etc. [13-27]. The nanoparticles within the polymer matrix do not form any coordination bonds but are stabilized by weak Coulombic or van der Waal's interactions. Their introduction into PANI may lead to electronic interactions, charge transfers, morphological modifications or a combination of these effects between the constituents of the nanocomposite system [28-31]. Such interactions amongst the constituents of the nanocomposite not only improve the existing properties but may also introduce interesting novel features [32]. For example, depending on the secondary component the nanocomposite can be multi-functionalized, as in the case of PANI/Fe_3O_4 nanocomposite which exhibit both conducting and magnetic character [33]. However, better dispersion of nanoparticles and an increase in interfacial interaction between the nanomaterial and PANI are integral for improvement in properties (thermal, electrical and optical). Another advantage of a nanocomposite lies in the fact that a very small amount of nanomaterial is generally sufficient to bring about the desired improvement in properties. Hence, the use of nanocomposite is also perceived as being economical.

In this review, we concentrate on the nanocomposites of PANI that have so far been prepared using different nanomaterials, and discuss the various strategies adopted for their preparation. We also focus on the potential applications of PANI nanocomposites in the area of gas

sensors and biosensors. Finally, we conclude with a discussion on future research strategies for PANI nanocomposites.

2. Synthesis of PANI Nanocomposites

The synthetic strategies for preparation of nanocomposites are of great importance as they impinge upon the resulting product in terms of morphology and properties, and consequently their applications. Most of the methods that are in use for nanocomposite preparation are generally based on two routes: (i) one-step redox reactions where simultaneous polymerization of aniline and formation of nanoparticle takes place or (ii) in situ polymerization where pre-synthesized nanoparticles are mixed into the monomer solution followed by chemical or electrochemical polymerization. Building on these two routes, nanocomposites have been prepared by both conventional and innovation approaches. In all the methods, however, one of the key criteria is the precise control of size and composition. Table 1 lists some of the synthesis methods employed in preparation of PANI nanocomposites, divided into categories based on nanomaterial type. These synthesis methods are discussed in detail expounding on the advantages and disadvantages of each method in the following section.

2.1. Nanocomposite of PANI with metal nanoparticles

The reversible doping/de-doping character of PANI can be used to advantage for the preparation of PANI/noble metal nanocomposites. As the standard reduction potential of most noble metal salts is higher than that of aniline, one-step redox reaction can be carried out to oxidize aniline with simultaneous reduction of the noble metal salts to give zero-valent noble metal nanoparticles. The resulting nanocomposite has the metal nanoparticles embedded into the PANI matrix. This method has been used to prepare nanocomposites of

PANI with Ag, Au, Pt, Cu, etc. [34-37]. Cho and coworkers [38] have fabricated PANI/Pt nanocomposite by interfacial polymerization in poly(styrene-sulphonic acid) solution with H_2PtCl_6 serving as both an oxidizing agent and a Pt precursor. The microscopy study suggested a correlation between the molar ratio of Pt and aniline monomer and the nanocomposite's morphology; while an excess of aniline concentration prompted secondary growth of PANI chains, a too small amount caused non-homogenous distribution of Pt nanoparticles in the polymer matrix. An alternative to chemical polymerization is electrochemical polymerization, as reported by Kinyanjui et al. [39]. Their investigation revealed a more uniform particle size of Pt formed as compared with electrochemical polymerization. While the redox synthesis method for insertion of nanoparticles into polymer matrix offers the advantage of composition control it is limited in it selection of metal precursors which are required to have a reduction potential higher than that of aniline.

In situ polymerization is another route to nanocomposite fabrication. It is the most commonly employed method because it provides a better size and shape control than the one-step redox method. Jing and coworkers [40] have reported an in situ chemical polymerization method for PANI/Ag nanocomposite with core-shell morphology. Barkade et al. [41] too employed the in situ polymerization route for nanocomposite preparation through ultrasound assisted miniemulsion polymerization of aniline in presence of pre-synthesized Ag nanoparticles. They reported the formation of PANI/Ag nanocomposite with small sized Ag nanoparticles (5-10 nm) embedded in the PANI matrix. The in situ polymerization technique allows local interaction between nanoparticles and the amine and imine units of PANI which consequently results in remarkably different and superior properties of the nanocomposite. Our group reported the synthesis of PANI/Ag nanocomposite via in situ chemical polymerization [42]. To ensure uniform dispersion of Ag nanoparticles in PANI matrix the nanoparticles were sonochemically dispersed in aniline hydrochloride solution followed by polymerization of

aniline by addition of APS. The TEM micrograph for the nanocomposite is presented in Figure 2. Microscopy studies indicated that ultrasound irradiation aided not only in uniform dispersion of nanoparticles throughout the PANI matrix but also effectively suppressed secondary growth of PANI thereby yielding nanofibers with small diameters of ~ 90 nm.

Metal nanoparticles can also be synthesized on the surface of PANI. Towards this end, stabilization of the nanoparticles by monomer is an interesting way to achieve monodipersed nanoparticles. Houdayer et al. [43] described a method for preparation of Ni/PANI nanocomposite for use as catalyst in Heck couplings. They first prepared zero-valent Ni particles by reduction of nickel acetate with sodium tert-butoxide activated sodium hydride in refluxing tetrahydrofuran (THF). A ligand exchange reaction with aniline gave aniline stabilized Ni particles. The composite was then prepared by polymerization of aniline with APS. Microscopy study revealed the Ni nanoparticles to be uniformly dispersed on the surface of PANI. The presence of such catalytically active metals on PANI surface makes the nanocomposite usable in catalytic applications. In yet another instance, Hosseini et al. [44] demonstrated fabrication of PANI/Pd nanocomposites by electroless method in which the Pd nanoparticles were deposited on the surface of PANI. This they accomplished by electro-polymerization of aniline on the surface of Ti electrode, and then immersing the PANI/Ti electrode in electroless-plating bath containing palladium (II) chloride, a complexing agent and a reducing agent. SEM micrograph of Pd nanoparticles deposited on PANI film is shown in Figure 3. Such uniformly dispersed nanoparticles in polymer matrix or on its surface is necessary to ensure optimum performance of the resulting nanocomposite in its field of application.

Template technique involving use of soft templates is yet another way to fabricate different nanostructures. Kong et al. [45] have reported synthesis of PANI/Pd nanotubes using polystyrene nanofibers as templates. The Pd nanoparticles were first coated with sulphonated

polystyrene nanofibers followed by PANI coating over it. The template nanofibers were then removed by dissolution in THF. The TEM images revealed that Pd nanoparticles were attached to the inner walls of PANI nanotubes. Although a facile way to prepare different nanostructures, the template technique poses problem in retaining the morphology due to the necessary template removal step.

2.2. Nanocomposite of PANI with metal oxide nanoparticles

Nanocomposites of PANI with metal oxide nanoparticles have the potential to serve as energy storage devices owing to the synergistic effect between the constituents. While the ICPs, such as PANI, serve as excellent electrode material having both electrochemical double layer capacitance and pseudocapacitance arising out of π–conjugated polymer chain, the problem of low conductance and volumetric shrinkage during ion ejection is addressed by the addition of metal oxides. Basavaiah et al. [46] described the fabrication of rod-like PANI nanostructures with nanoparticles of magnetite via micelle-assisted one pot synthesis. They first added a mixture of ferric chloride and ferrous sulphate solution to DBSA-doped PANI solution and followed it with addition of ammonium hydroxide at high temperature.

In certain synthesis methods, the PANI is grown on the surface of the nanoparticles. Zhu et al. [47] have reported a two-step process for synthesis of PANI/ZnO nanograss. Their method involved chemisorption of PANI on the surface of hydrothermally grown ZnO on fluorine-doped tin oxide (FTO) substrate. A schematic of synthesis procedure for nanograss formation along with their FE-SEM micrograph is presented in Figure 4. It was observed that the deposition of PANI on ZnO nanostructure with high aspect ratio did not alter the latter's morphology thereby rendering the hybrid system suitable for solar cell performance.

Researchers have also used surfactants as soft templates in order to obtain composite nanostructures. Wang and coworkers [48] reported the synthesis of TiO_2/PANI core-shell

structure using different surfactants as soft templates. They noted that the type of surfactant influenced the morphology of the nanocomposite. The SEM images revealed the formation of core-shell morphology facilitated by the surfactants which enhanced the interfacial interaction between the TiO_2 surface and aniline hydrochloride. Several reports of template-free synthesis methods for fabrication of PANI nanocomposites can be found in literature [49-53]. We reported the fabrication of PANI/γ-Fe_2O_3 nanocomposite via in situ polymerization method using a binary dopant system involving protonic acid and a surfactant [54]. Our investigations demonstrated that the binary dopant system not only increased charge density in the polymer but also influenced the PANI's size and morphology. The SEM images, shown in Figure 5, revealed that the γ-Fe_2O_3 nanoparticle content not only affected the diameter of the PANI nanofibers but also promoted secondary growth of PANI.

Oxidant or initiator free synthesis of PANI nanocomposite can also be found in literature. Nanobelts of PANI/V_2O_5 composite with core-shell morphology were prepared in which V_2O_5 itself acted as a template as well as oxidant for aniline polymerization [55]. Typical of aniline self-assembly, the morphology was found to be influenced by pH of the solution. These same constituents, prepared under different reaction conditions, can yield different morphologies. Pang and coworkers [56] reported nanocomposite formed by intercalation of PANI chains between layered V_2O_5 through in situ polymerization under hydrothermal conditions. Here again, the microscopic studies suggested that the reaction conditions influenced the morphology of the nanocomposite. For example, nanosheets were formed at high temperature whereas at room temperature rod-like aggregates were obtained. In this case, self-assembly of nanosheets resulted in tremella-like structure. The effect of synthesis method as well as synthesis parameters resulting in morphological variations involving the same set of constituents has been recorded by many researchers.

A somewhat different approach to nanocomposite fabrication was taken by Rao and Vijayan [57]. They synthesized PANI/RuO_2 nanocomposite via chemical oxidation of ruthenium (II)-tetraaniline complex by H_2O_2 in presence of HCl. NMR spectroscopic analysis indicated the formation of a tetraaniline complex along with reduction of Ru(III) to Ru(II). Oxidation with H_2O_2 resulted in simultaneous formation of PANI and RuO_2 with sponge-like morphology.

Nanocomposites have also been prepared by physically mixing PANI with nanoparticles. Patil and co-workers [58,59] have demonstrated that the optical property of the physical mixture of PANI/ZnO nanocomposite is much different from its constituents. As sensors, these nanocomposites also exhibited superior performance than their constituents.

2.3. Nanocomposite of PANI with CNT or graphene

Graphenes are atom thick layers of carbon exhibiting exceptional properties. Theses layers or sheets when rolled at specific chiral angles form carbon nanotubes (CNT). CNTs possess extremely high aspect ratio, and show extraordinary thermal, electrical and mechanical properties, which are dependent on the rolling angle and radius. When incorporated into PANI they improve its properties and also render it useful in various applications. Deposition of PANI layer onto 1D CNT nanostructure is the simplest method of nanocomposite preparation, and is often achieved by attaching functional groups on the CNT surface or using surfactants. Zhang et al. [60] have described an in situ polymerization synthesis of PANI/CNT nanocomposite with cable-like structures using the cationic surfactant CTAB. Microscopic studies suggested that the formation of PANI took place on the surface of MWCNT and that the cable-like structures were a result of CTAB directed self-assembly of PANI. The Raman spectroscopic studies indicated a site-selective interaction of CNT with PANI moieties. Such observation has been made by several researchers in case of in situ polymerization.

Similar to CNTs, graphenes too are incorporated into PANI to obtain nanocomposite with superior electroactivity. The use of surfactant in these cases is to facilitate exfoliation of graphene sheets in the PANI matrix. Vega-Rios et al. [61] demonstrated the use of anilinium dodecylsulphate both as a surfactant and a monomer; polymerization of aniline took place directly over the flake-like graphene structures. The advantage of the in situ technique lies in its adaptability to a number of methods for nanocomposite preparation, as has been demonstrated by several research groups [62-64].

Electrospinning is another method for fabricating PANI/CNT nanocomposite [65,66]. Highly aligned nanofibers can be obtained by controlling electrospinning parameters such as applied voltage, speed of rotating mandrel, distance between tip and collector, etc. Shin and coworkers [67] reported the fabrication of nanocomposite of CNT with a blend of PANI/PEO by electrospinning. Microscopic study revealed the highly aligned nature of the nanocomposite with the MWCNTs dispersed inside the PANI matrix. The highly aligned MWCNTs inside the PANI matrix imparted the nanocomposite a significantly high conductance value. Although the process of electrospinning is cumbersome due to the large number of variables controlling the product morphology, it nevertheless remains a process of choice to produce highly aligned electrospun mats and nanofibers.

Functionalization of CNTs prior to nanocomposite formation is yet another variation in synthesis technique which ensures a strong interaction between CNT and the polymer thereby facilitating charge transfer. Kar and Choudhaury [68] described the effect of functionalized CNTs on the resulting nanocomposite with PANI. They prepared CNT/PANI nanocomposite by incorporating carboxylic acid functionalized MWCNT into PANI. The morphological analysis (Figure 6) showed a well embedded CNT in PANI matrix suggesting that surface modification of MWCNT with carboxylic acid functional groups improved their dispersion in the monomer solution leading to enhanced interaction between the matrix and CNT.

Furthermore, Raman spectroscopic study revealed that the strong interaction between the functionalized MWCNTs and PANI chains resulted in electron delocalization, and hence, doping of PANI by the CNTs.

In case of graphene too, researchers have endeavoured to address the challenge of incorporation of graphene into PANI without sacrificing its conducting nature. In one method, diazotization followed by amination of graphene sheet is carried out prior to covalently grafting it with PANI in order to prevent damage of graphene sheets and their aggregation [69]. While the carboxylic and hydroxyl groups on the GO surface enhance interfacial interactions with the polymer matrix, they also make it non-conducting which limits their application. The formation of amine functional groups not only increased the conductivity of graphene but also retained nucleation sites for aniline polymerization. In yet another study, nanocomposite was prepared by polymerization of aniline on the surface of poly(styrenesulphonic acid) functionalized graphene [70]. Interestingly, this poly(styrenesulphonic acid) coated graphene was found to effectively dope PANI. Moreover, the resulting nanocomposite was readily dispersible in water.

Graphene oxide (GO) too have been used in PANI matrices. Sandwich-like morphology of GO/PANI has been obtained when prepared in absence of surfactants [71]. In fabrication of GO/PANI nanocomposite by in situ polymerization Huang and Lin [72] reported that reaction pH greatly influenced the morphology of the resulting nanocomposites - while low acidity yielded nanotubes and nanospheres, aligned nanofibers were obtained at high acidity levels. Preparation of nanocomposite by polymerization of aniline in presence of GO and further reduction by hydrazine hydrate has been described by Li et al. [73]. These nanocomposites were found to have high adsorption capacity of Hg (II) in aqueous solutions.

2.4. Nanocomposite of PANI with chalcogenides

Chalcogenides are compounds of sulphides, selenides and tellurides. When combined with PANI they significantly improve its optical property to a large extent. Nanocomposites of PANI and chalcogenides (such as CdS, ZnS and CdSe) have potential application in energy devices and sensors. Ameen et al. [74] described the formation of CdS on the surface of PANI nanorods. They first prepared DBSA doped PANI and then synthesized CdS nanoparticles in the same polymerization reaction mixture by co-precipitation. The synthesized nanocomposite exhibited improved electrochemical behaviour. An in situ technique for CdS/PANI preparation was described by Raut et al. [75] where CdS was first prepared by sol-gel technique, followed by polymerization of aniline. The nanocomposites were found to have a lower band gap than neat PANI. Similar reports of PANI/ZnS and PANI/CdSe can be found in literature [76,77]. Haldorai et al. [78] reported a two-step ultrasound assisted dynamic inverse microemulsion method for nanocomposite preparation of PANI with CdSe quantum dots. The TEM images revealed uniformly dispersed CdSe quantum dots of an average size of 5 nm in the PANI matrix. The nanocomposite formed had high thermal stability as compared to neat PANI. The combination of PANI and CdSe lowers the latter's luminescence lifetime.

2.5. Nanocomposite of PANI with phthalocyanines and porphyrins

Phthalocyanines are macrocyclic compounds with metal centers (coordination complex), while porphyrins are heterocyclic macrocycles containing four pyrrole subunits interconnected by methane bridges. Porphyrins, in general, exhibit good photoluminescence and electrocatalytic properties. Their incorporation into PANI decreases its conductivity but their nanocomposites find applications in fields like sensors and light emitting diodes. Synthesis of hybrids of PANI with tetrasulphonated metal phthalocyanins by LBL technique

can be found in literature [79,80]. Zucolotto and coworkers [79] reported nanocomposites of PANI with sulphonated pthalocyanines prepared by LBL technique. The FTIR spectroscopic study indicated towards a molecular-level interaction between the metal ion containing phthalocyanines and PANI. Porphyrins too are used in PANI for sensing of compounds [81]. Zhou et al. [82] reported the preparation of PANI/cobalt-porphyrin nanocomposite by one-step electrochemical synthesis. Microscopy study revealed a porous structure with nanorods of Co-porphyrin. They demonstrated the formation of J-aggregates in acidic aqueous solution that served as templates for electropolymerization of aniline. The combined properties of the two components in the nanocomposite render it multifunctional for applications in diverse fields.

2.6. Nanocomposite of PANI with polymers

Polymers such as polyvinyl alcohol (PVA), polyvinyl acetate (PVAc) and polymethyl methacrylate (PMMA) have been extensively made into nanocomposites with PANI. The incorporation of these polymers induce thermal and mechanical stability as well as processability. An in situ method for composite formation using PVA hydrogel has been reported by Adhikari and Banerjee [83]. The method involved immersing APS soaked PVA hydrogel into aniline hydrochloride solution leading to formation of PANI in the bulk and on the surface of PVA. A similar approach was taken by Bajpai et al. [84] for preparing PANI/PVA nanocomposite. Another in situ technique has been offered by Arenas and coworkers [85] for formation of aqueous suspension of PANI/PVA system, which involved the use of a surfactant or an organic acid to improve solubility of the nanocomposite. Patil et al. [86] too prepared a highly stable PANI/PVA film by a two-step process. First, a PVA solution was spin coated on a FTO substrate and then PANI was dip coated onto this substrate by aniline polymerization. The nanocomposite film showed excellent

electrochemical stability without any loss of specific capacitance. Araujo et al. [87] described a two-step method for preparation of nanocomposite of PANI with PMMA. PANI nanofibers synthesized by interfacial polymerization were sonochemically dispersed butanone and then mixed with PMMA/butanone solution. This was followed by solution casting this mixture to obtain the nanocomposite film.

Electrospinning was employed by Panthi and coworkers [88] for preparation of PANI/PVAc nanocomposite mats. They, however, first individually dissolved PANI and PVAc in THF and DMF, respectively, and then mixed the two solutions and electrospun using silicon substrate as a collector. PANI/PMMA fibers were also prepared by electrospinning, as demonstrated by Veluru et al. [89]. They prepared PANI by chemical polymerization at low temperature, and then mixed it with CSA in chloroform in a homogenizer for several hours. This PANI solution was then mixed with PMMA and electrospun. As discussed before, the process of electrospinning allowed controlling fiber morphology to yield highly aligned fibers.

2.7. Nanocomposite of PANI with multi-components

PANI nanocomposites with multi-components (more than one type of nanomaterial) have been prepared in order to obtain multi-functional materials which show different properties (like electrical, optical and magnetic property) within the single material, or induce significant improvement in an existing property. Such hybrid materials, consequently, project a greater scope of applications. The most widely prepared PANI multi-component systems are based on PANI/CNTs. A graphene/PANI/CNT double-layer capacitor with hierarchical structure has been fabricated by Lu et al. [90]. In the first stage they prepared PANI/CNT by in situ polymerization. In the next stage, the PANI/CNT dispersion was mixed with an aqueous dispersion of GO via sonication. After several hours, the flocculated mixture of

GO/PANI/CNT was stabilized by adjusting its pH, and then centrifuged to obtain GO/PANI/CNT precursor. This was followed by reduction of GO to graphene by hydrazine gas. The reduced PANI was then re-doped to restore its electrical conductivity. Microscopic studies, as shown from SEM and TEM images in Figure 7, showed uniform encapsulation of CNT by PANI forming ID core-shell nanostructures. The researchers also demonstrated that the GO sheets facilitated stable dispersion of PANI/CNT nanocomposite. Fabrication of hybrid material from graphene, PANI and CNT has been reported by other research groups as well using different synthetic techniques [91-93].

Another type of hybrid composite is based on PANI/CNT with a magnetic material. Wang et al. [94] prepared a PANI/Fe_3O_4/CNT composite for protein digestion by depositing Fe_3O_4 on CNTs, followed by in situ polymerization of aniline in presence of trypsin. The trypsin immobilization on the composite allows for protein analysis while the superparamagnetic behaviour, due to the presence of Fe_3O_4, facilitates its isolation from the digests when an external magnetic field is applied. We demonstrated the fabrication of PANI/γ-Fe_2O_3/CNT hybrid nanocomposite deposited on cotton fibers for sensing application. The strategic protocol described by Shimpi et al. [95] for fabrication of the hybrid material involved serial immersion of cotton thread firstly in a CNT colloidal solution and then in a dispersion of PANI/γ-Fe_2O_3 nanocomposite under ultrasonic irradiation. Microscopic studies revealed deposition of CNT onto the cotton thread with PANI/γ-Fe_2O_3 uniformly distributed over them. Nanocomposites of PAN/CNT with a tertiary component of magnetic or semiconducting nature have also been reported [96,97]. Depending on the synthesis conditions these nanostructures can have different morphologies, and also exhibit properties vastly different from the individual components.

Multi-component systems of PANI with metal oxides can also be found in literature. A hybrid nanocomposite based on SnO_2-ZnO/PANI for NO_2 sensing has been made by Xu et al.

[98] where the presence of both SnO_2 and ZnO had implications for the response towards NO_2. In this case, a solvothermal hot press route was adopted for the preparation of SnO_2-ZnO porous nanoparticles. An alumina tube was then coated with a thick paste of SnO_2-ZnO composite and sintered. Finally, nanocomposite was prepared by applying a paste of PANI with NMP over the SnO_2-ZnO porous nanosolid thick film.

Boomi and co-workers [99-101] prepared a series of multifunctional nanocomposites of PANI with different bimetallic nanoparticles by chemical method. These hybrid nanocomposites show better thermal stability (PANI/Ag-Pt) than neat PANI, as well as antibacterial effect. Fe_3O_4-Au/PANI multifunctional nanocomposite has been synthesized by in situ chemical polymerization in presence of mercaptocarboxylic acid, which acted as a template for the rod-like structures [102]. The optical, electrical and magnetic properties exhibited by the nanocomposite were dependent on the molar ratio of Au to Fe_3O_4.

Lee et al. [103] have reported a PMMA/PANI/Ag nanocomposite prepared by coating of PMMA spheres with PANI via in situ chemical polymerization, followed by electroless coating of Ag. The presence of PANI on the PMMA surface facilitated efficient plating of Ag due to high the activation effect. The nanocomposite showed greater thermal stability, and its electrical conductivity increased with Ag content.

Nanocomposite of polyaniline with a blend of other polymers is an economical way to achieve conductivity in polymers. Li et al. [104] have prepared PANI/PMMA/PU nanocomposite with core-shell morphology through a two-step polymerization process. In the first step they prepared spheres of PU-PMMA by miniemulsion polymerization using SDS. In the second step a shell of PANI was given over the PU-PMMA core by chemical polymerization of aniline with HCl and DBSA as dopants. Variation in the concentration of dopants yielded different morphologies for PANI. Moreover, increasing concentration of DBSA was responsible for higher electrical conductivity of the nanocomposite as it

facilitated better coverage of PANI over the core. Similar nanocomposite of PU-PMMA filled CSA-doped PANI in the form of interpenetrating network (IPN) has been prepared by Jeevananda and Siddaramaiah [105]. The morphological analysis of the IPN system revealed two different phases pertaining to the PU and PMMA in the system.

3. Sensing Applications of PANI Nanocomposites

A sensor is a device which detects and measures a physical quantity and then provides a readable output for it. A sensor's *response* is the measure of a change in its physical parameter resulting from some chemical stimulation [106]. Figure 8 shows a general response curve for a sensor where x-axis represents 'activity of analyte' and the y-axis represents 'transduction function'. The sensor response varies in the dynamic range, and then saturates beyond the saturation limit. Factors such as reliability, reversibility and selectivity are important in the context of practical applicability of a sensor. Ideally, a sensor response should be reversible, and the sensor should show high selectivity, i.e., it should respond only to one analyte even in the presence of other interfering species.

PANI is the most important candidate in the field of sensors. As a sensing element it allows monitoring and detection of various analytes in ambient condition (room temperature), which is a safer option compared to sensors operating at high temperatures. Its interaction with analytes influences its redox properties, leading to a change in its resistance, work function or electrochemical potential [107]. Immobilization of enzyme or other biological agents on PANI or its nanocomposites is also possible which extends its ambit as a biosensor. Despite its many merits it suffers from low sensitivity and poor selectivity. This issue is often addressed by addition of a secondary component into PANI, which can induce sensitivity or selectivity in PANI, either through effective interaction with PANI or by simply acting as a catalyst. Table 2 presents a list of various PANI based nanocomposites with potential

application as gas sensors or biosensors. An in-depth discussion on these PANI based sensors is provided in the following sections.

3.1.PANI Nanocomposites as Gas Sensors

Commercially available gas sensors based on metal oxides generally operate at high temperatures. This causes structural changes in the sensing material resulting in instability and response variation. Another risk pertains to the detection of combustible gases or gas mixtures that might auto-ignite at high temperatures. PANI based sensors allow safer detection of a number of combustible gases in ambient conditions (room temperature). The performance of PANI sensors can further be improved by inclusion of nanoparticles which induces sensitivity and selectivity in PANI. Other criteria affecting PANI performance is the its physical form - thin films exhibit higher sensitivity to analytes as compared to pellets. Moreover, nanofibrillar network of PANI through self-assembly gives porous structure caused by features of solid-state polymerization. This structure permits penetration of gaseous molecules into the polymer film from the environment. The diffusion of gas molecules into the polymer and their adsorption onto nanoparticles modifies its electrical behaviour. This is particularly significant in nanocomposite materials whose conductivity is governed by electron transfer between nanoparticles and polymer. Hence, a strong sensor effect is observed in case of PANI nanocomposites resulting from a marked influence of low molecular weight gaseous analytes. Therefore, adsorption of analyte molecules on the sensor surface is the first step leading to their detection, and has been experimentally studied as well [107]. Other factors influencing the response of nanocomposites towards analytes are morphology, size, surface area, and nanoparticle content. In the following sections we discuss PANI based nanocomposite sensor designed for different classes of gaseous analytes.

3.1.1. VOCs sensor

Alcohols have a wide range of applications, from solvents and preservatives to antiseptics and fuels. However, alcohol vapour inhalation can have serious health implications as well. Extensive work has been done in detection of alcohol vapours using metal or metal oxide inclusions into PANI matrix. Athawale and co-workers [108] reported detection of methanol by PANI/Pd nanocomposite. Their investigation revealed a very high response, to the order of ~ 10^4 magnitudes, for saturated levels of methanol vapour. FTIR spectroscopic study indicated that Pd inclusions act as a catalyst for reduction of imine nitrogens in PANI by methanol. Moreover, in a mixture of VOCs, the PANI/Pd nanocomposite selectively detected methanol with an identical magnitude of response but at a longer response time. Catalytic influence of Ag nanoparticles embedded in PANI matrix in ethanol detection has been reported by Choudhury [109]. He demonstrated that faster protonation-deprotonation of PANI takes place on exposure to ethanol in presence of Ag nanoparticles.

More recently, PANI/Ag nanocomposite has been employed for detection of triethylamine and toluene [110]. They proposed a chemisorption and diffusion model for the sensor response. While they asserted that the sensor response towards triethylamine and toluene is a result of both deprotonation of PANI and swelling of the polymer by the analyte causing a drop in its conductivity, it could not be definitely ascertained which of the two pathways was dominant.

Chloroform is a widely used solvent and an anaesthetic. It is also an irritant and can cause depression of central nervous system upon inhalation. Chloroform monitoring has been reported by Sharma et al. [111] using PANI/Cu nanocomposite. They suggested an adsorption-desorption phenomenon at the surface of metal clusters as a possible mechanism. The FTIR spectroscopic study suggested interaction of chloroform with metal clusters. PANI nanocomposites with nanometal inclusions exhibit superior performance than neat PANI in

detection of VOCs. These investigations, however, point towards a catalytic pathway as the underlying mechanism.

3.1.2. Sensors for reducing gases – NH_3 and H_2S

PANI sensor for detection of reducing gases, such as NH_3 and H_2S, is one of the most researched areas since the underlying sensing mechanism is straightforward, i.e., deprotonation of PANI when exposed to reducing gases through electron donation by the latter, resulting in increased resistance of PANI. Introducing a secondary component further adds to this feature advantageously as it serves to enhance the sensitivity of the sensor or improve its selectivity, or both. Detection of reducing gases by PANI/metal oxide nanocomposites has been extensively studied by various research groups. Metal oxide nanoparticles, when combined with PANI, forms p-n heterojunction with a depletion layer. Adsorption of gases brings out about a change in this depletion region which manifests itself as a change in its electrical property. Pawar et al. [112] reported a highly selective NH_3 sensor based on PANI/TiO_2 nanocomposite. The thin film sensor exhibited gas response towards an NH_3 concentration as low as 20 ppm. They proposed that the response was owing to creation of a positively charged depletion layer at the heterojunction of PANI and TiO_2. Similar observations on NH_3 detection were made by Dhingra et al. [113]. A different observation, however, was made by Deshpande and coworkers [114] who studied the response of PANI/SnO_2 nanocomposite towards NH_3. They found that while neat PANI gets reduced in NH_3 environment, the nanocomposite shows an oxidized characteristic in presence of the gas. The I-V characteristic of the nanocomposite, shown in Figure 9(c), revealed a diode-like character which is associated with electrical conductance through hopping mechanism. The n-type SnO_2 expunges the holes in PANI through formation of localized p-n heterojunction thereby making the PANI/SnO_2 nanocomposite electrically more insulating in

nature. However, exposure to NH_3 gas caused polarization of NH_3 molecules by the depletion region, which provided PANI molecules with positive charge whose mobility along the PANI chain made the nanocomposite relatively more conducting. The formation of such p-n heterojunction between PANI and nano-metal oxide has been proposed by other research groups as well [59,115].

Zhang and coworkers [116] reported PANI/PMMA nanocomposite for trace level NH_3 detection for concentration as low as 1 ppm. The high sensitivity of the sensor was attributed to the highly aligned PMMA microfibers coated with PANI which facilitated faster diffusion of gas molecules, thereby accelerating electron transfer. Very recently, Zhihua and coworkers [117] reported a porous thin film nanocomposite of PANI/sulphonated Ni phthalocyanine for NH_3 sensing. They demonstrated that Ni phthalocyanine catalyzed electrodeposition of PANI films which in turn adversely affected the sensor's performance.

Detection of H_2S gas using PANI nanocomposites has also been successfully attempted. Crowley and coworkers [118] developed PANI/$CuCl_2$ sensor printed on screen printed interdigitated electrodes for trace level H_2S detection. A very different phenomenon was observed in their study, i.e., exposure to H_2S gas resulted in protonation of PANI nanocomposite. The researchers proposed that PANI gets deprotonated by complexation with $CuCl_2$. When exposed to H_2S gas, preferential binding of $CuCl_2$ with S^{2-} ion resulted in evolution of HCl which protonated PANI increasing its electrical conductivity. A similar study based on PANI/$CuCl_2$ printed on interdigitated electrodes for H_2S detection was carried out by Sarfaraz et al. [119] as well. Raut and coworkers [120] demonstrated the use of PANI-CdS nanocomposite film for room temperature detection of H_2S gas wherein they achieved a maximum response of ~ 48% for 100 ppm H_2S concentration. They reported the sensing mechanism to be dominated by the modifications at the depletion region.

Shirsat et al. [121] have proposed a mechanism involving the formation of AuS (Eq.1) and subsequent protonation of PANI for H_2S detection by PANI/Au nanocomposites.

$$H_2S + Au \rightarrow AuS + 2H^+ \qquad (1)$$

They suggested that donation of electrons to the protons formed in the reaction (Eq.1) led to a change in the resistance of the PANI/Au nanocomposite. Figure 10 shows the response of PANI/Au nanocomposite and PANI as a function of time towards different concentrations of H_2S gas. The nanocomposite exhibited excellent response to trace level H_2S gas (~ 0.1 ppb). The authors suggested that transfer of electrons from PANI to Au led to a drop in resistance of the material.

3.1.3. LPG sensor

LPG sensing by PANI nanocomposites is also a much investigated topic. An inflammable gas such as LPG demands detection in ambient conditions (i.e., at room temperature) for safety purposes. The use of electroactive PANI as a physical transducer for room temperature sensing provides a safer option as opposed to metal oxide based high temperature detectors. Joshi et al. [122] reported the use of n-CdSe/p-PANI nanocomposite for LPG sensing wherein the response was a result of the sensor's modified depletion layer. In a similar vein, we reported the detection of LPG by PANI/γ-Fe_2O_3 nanocomposite at room temperature [54]. Microscopic study revealed nanoscale morphology for the nanocomposites which afforded a high surface area for gas adsorption. I-V characteristic of the nanocomposite, as shown in Figure 11, revealed the formation of a p-n heterojunction between PANI and γ-Fe_2O_3 nanoparticles. Based on our investigations, we proposed that the detection of LPG resulted from an increase in the depletion depth due to the adsorption of gas molecules at the depletion region of the p-n heterojunction. Moreover, the sensor's response was found to be influenced by the nanoparticle content.

Dhawale and coworkers [123-125] prepared a series of PANI based nanocomposite sensors for detection of LPG at room temperature. Their sensors exhibited significant selectivity towards LPG as compared to N_2 and CO_2. They too ascribed the sensor's response to a change in the barrier potential of the heterojunction.

3.1.4. Humidity sensor

Humidity (water vapour) has significant effect on electrical conductance of PANI. Its detection using PANI based sensors is another arena where extensive research has been conducted. Shukla et al. [126] reported a PANI/ZnO nanocomposite based electrochemical humidity sensor. They suggested that adsorption of water molecules on the sensor surface causes efficient directional charge conduction at the heterojunction formed between PANI and ZnO. They found that charge conduction becomes more profound in case of PANI/ZnO nanocomposite as ZnO increased water adsorption capacity of PANI. Vijayan et al. [127] have reported an optical fiber based PANI/Co humidity sensor which exhibited very low response and recovery times of 8 s and 1 min, respectively. In yet another case, PANI/Ag nanocomposite deposited on an optical fiber clad was used for humidity detection [128]. A dramatic improvement in sensor response was observed with reduction in size of Ag nanoparticles. Such high responses towards humidity have been observed with other PANI nanocomposites as well [129,130]. A fast responsive humidity sensor based on a hybrid nanocomposite structure of PANI with silver-vanadium oxide has been reported by Diggikar et al. [131]. Because PANI is significantly affected by humidity, detection of other analytes in the presence of humidity does not allow real time monitoring. In their recent work, Cavallo and coworkers [132] have demonstrated that at high level of relative humidity (65-90%) swelling of polymer due to continuous absorption of water takes place, which increases its interchain distance thus hindering the charge hopping process and decreasing electrical

conductance. It is therefore imperative that the influence of humidity on the electrical behaviour of PANI and its pathways be investigated.

3.1.5. Other gases

PANI has low sensitivity towards certain gasses, such as methane (CH_4) and carbon monoxide (CO), as these do not show redox properties at room temperature. Such analytes may not undergo chemical reactions with polymers, but have weak physical interaction with the polymer matrix. The presence of metal/metal oxide nanoparticles in the PANI matrix can enhances its response towards these gases. Indium (III) oxide (In_2O_3) incorporated PANI nanocomposite exhibited good responses towards CH_4 and CO [133]. The response was higher for CH_4 and was found to be temperature dependent. The theory of analyte detection via catalytic pathway has also been proposed by Ram et al. [134] in their study of CO detection by PANI/SnO_2 nanocomposite. PANI/SWCNT nanocomposite based sensor too demonstrated good response towards CO [135]. As compared to NH_3 gas which was also included in the study, the sensor showed propensity towards CO absorption. In most cases, detection of CO by PANI nanocomposite is explained using the particle electron transfer model – the stable resonance structure of $^{+}C{\equiv}O^{-}$ withdraws the lone pair of electron from the amine nitrogen in PANI thus creating a positive charge on it. The mobility of these positive charges generated on the amine nitrogen of PANI increases its conductivity.

PANI/TiO_2/MWCNT nanocomposite has been successfully used for NO detection through photocatalytic behaviour of TiO_2 [136]. The authors reported that under UV irradiation the NO gas gets decomposed under the photocatalytic effect of TiO_2 giving HNO_2, NO_2 and HNO_3. These decomposition products get adsorbed onto the surface of PANI/MWCNT, owing to its high specific surface area and hydrophilicity of PANI. Such combination effects changes the electrical resistance of the nanocomposite, thus facilitating detection. Figure 12

shows the sensitivities (S) of the nanocomposites towards NO under UV irradiation. PANI/TiO_2/MWCNT nanocomposite (PCT) exhibited a high response towards NO, while PANI (PA) showed the least. PANI/MWCNT (PC) and PANI/TiO_2 (PT) composites showed better response as compared to its individual components.

Several other gases such as NO_2 and H_2 were also detected by PANI nanocomposites [98,137,138]. Introduction of CNT or metal oxides into PANI have shown response towards H_2 gas. Srivastava et al. [138] used interdigitated electrodes based on PANI/TiO_2 and PANI/MWCNTs for H_2 gas detection with both the materials eliciting a high response. Arsat et al. [139] too reported PANI/MWCNTs deposited on lithium tantalite SAW transducers for H_2 gas detection. Another SAW based PANI/WO_3 sensor deposited on layered ZnO/64° YX $LiNbO_3$ SAW transducer gave fast response with good repeatability [140]. A PANI/PtO_2 based thin film sensor has also been reported for H_2 sensing [141]. The authors reported that the PtO_2 present in PANI was reduced to PtO during sensor conditioning stage. When the sensor was exposed to H_2 gas, it catalytically oxidizes to water which decreases the resistance of PANI.

Azim-Araghi and Jafari [142] developed an interdigitated electrode of PANI-chloroaluminium phthalocyanine (PANI/ClAlPc) for CO_2 detection. They reported an optimum concentration of 10% for ClAlPc in PANI for maximum sensitivity at 300 K. They proposed the formation of a charge transfer complex between the aromatic units in PANI and phthalocyaninie as donors with CO_2 acceptor molecules.

The detection of a single analyte can take place through several different pathways – from nanometal catalyzed reaction to modification of barrier height. The response elicited from a nanocomposite sensor on exposure to an analyte is governed by two factors: (i) charge transfer phenomenon between the constituents of the nanocomposite, and (ii) reaction between the analyte and the nanocomposite. For example, as previously discussed, H_2S can

either have a reducing or an oxidizing effect on PANI depending on the interaction of PANI with the secondary component in the nanocomposite. Moreover, taking into account the humidity factor is necessary as it is known to significantly decrease the sensitivity of PANI sensors. Therefore, for future PANI based sensing materials, a deeper understanding of the sensing behaviour is required to develop high performing sensors.

3.2. PANI Nanocomposites as Biosensors

Updike and Hicks [143] reported the first biosensor system which functioned through immobilized sensor activity. This was the beginning of modern biosensors that are widely in use today. Their system comprised of an enzyme (glucose oxidase) immobilized on a gel which measured the concentration of glucose in biological solutions. A variety of biosensors has come up since, finding applications in industry, clinical diagnostics and environment monitoring [144].

A biosensor typically consists of a biorecognition element (or bioreceptor), a transducer element, and electronic components for signal processing. The schematic of a biosensor operation is shown in Figure 13. It operates in three stages - (i) recognition of a specific analyte by the bioreceptor, (ii) transformation of biochemical reaction into transducer-type reaction, and (iii) processing of transducer signal [144].

PANI is particularly attractive as biosensors as it provides a conducting matrix for immobilization of bioreceptors (i.e., confined movement of bioreceptors in a defined space) onto it. Its electroactivity allows it to act as a mediator for electron transfer through a redox or enzymatic reaction. Such direct communication with the bound bioreceptors leads to a range of analytical signals which gives a measurement of the sensor activity [145]. Apart from its electronic properties, PANI has shown excellent stability and strong biomolecular interactions [146,147] necessary for biosensor applications. Properties of PANI such as

electrical conductivity, electrochromism and pH sensitivity have been successfully employed for detection of different biological compounds [148-150]. Nanocomposites of PANI provide a scope to further assess the potential of these materials as biosensors. A secondary component in the PANI matrix is often seen to increase bioreceptor binding onto PANI surface. Based on the bioreceptors, biosensors are broadly classified as enzymatic biosensors, immunosensors, and DNA/nucleic acid biosensors, which are discussed in the following sections.

3.2.1. Enzymatic biosensors

The concept of enzymatic biosensors was introduced by Clark and Lyons [151] using the enzyme glucose oxidase (GOx). They developed an amperometric biosensor in which the enzyme catalyzed the oxidation of glucose on the surface of Pt electrode. Owing to the enzymatic reaction the oxygen flux to the electrode surface varied as a function of glucose concentration, thus enabling its detection. However, the enzyme activity took place in solution as opposed to the recent biosensors which have immobilized enzymes.

3.2.1.1. Glucose biosensor

Since it was first introduced, glucose biosensors have undergone significant modifications as regards to its detection technique and development of newer materials for enzyme immobilization. Xian et al. [152] have reported a glucose biosensor based on Au/PANI nanocomposite. GOx and Nafion were immobilized on the nanocomposite surface, and quantification of glucose was done by electrochemical detection (oxidation) of enzymatically released H_2O_2. A much higher anodic current was observed by the Au/PANI nanocomposite as compared to PANI, indicating a better response, possibly as a result of electron transfer between electrode and H_2O_2 facilitated by Au in PANI matrix. Xu et al. [153] prepared a

graphene/PANI/Au nanocomposite modified GCE[1] as glucose biosensor. This nanocomposite was found to be more biocompatible and facilitated efficient electron transfer between GOx and the electrode.

Nanocomposites of PANI/MWCNTs have also been employed as biosensors for glucose detection [154-156]. The biosensor developed by Le et al. [156] had PANI/MWCNTs deposited on interdigitated planar Pt-film electrode over which the GOx was immobilized via glutaraldehyde. Figure 14 presents the graph showing rapid amperometric response of PANI/MWCNTs to changing glucose concentration. The porous nature of the nanocomposite facilitated stronger binding to GOx, and the nanocomposite proved to be an efficient transducer with a response time of 5s. More recently, Zhu and coworkers [157] reported a GOx immobilized PANI-TiO_2 nanotube composite as electrochemical biosensor. The performance studies revealed that the nanoscaled tub-like morphology facilitated direct electron transfer of GOx, giving a sensitivity of 11.4 μA mM^{-1} at a low detection range of 0.5 μM at a high signal-to-noise ratio.

Though most biosensors utilize immobilized GOx for glucose detection, other enzymes can also be used for this purpose. Ozdemir et al. [158] have reported a biosensor based on pyranose oxidase immobilized Au/PANI/AgCl/gelatin nanocomposite for glucose detection, wherein sensing was facilitated by amperometric detection of consumed O_2 during the enzymatic reaction. The importance of glucose biosensors lies in simplistic and accurate monitoring of blood glucose levels, which might help in controlling the growing issue of diabetes around the world.

[1] Glassy carbon electrode

3.2.1.2. Cholesterol biosensor

The rise in heart diseases and other illness related to high cholesterol levels in blood has prompted researchers to develop suitable devices for efficient and accurate monitoring blood cholesterol levels. Towards this end, a number of publications cite PANI nanocomposites as a material conducive to cholesterol detection. For instance, Srivastava et al. [159] reported a cholesterol oxidase (ChOx) immobilized PANI/Au/chitosan nanocomposite for cholesterol detection. The enzyme-substrate kinetics for the nanocomposite biosensor showed that it facilitates enzymatic reaction and activity. PANI nanocomposites with CNTs and/or graphene are also extensively used for cholesterol detection. A ChOx immobilized graphene/PVP/PANI modified paper-based electrode has shown a low detection limit of 1 μM^2 [160]. The presence of PVP was reported to enhance the sensitivity of the biosensor.

It has often been observed that these biosensors show a high shelf life when stored at low temperature. PANI/Ag nanocomposite too was employed as cholesterol sensing [161]. The biosensor gave a fast response towards cholesterol and showed uniform activity for up to 50 days when stored at low temperatures. Dhand et al. [162] have described a PANI/MWCNT coated ITO electrode over which ChOx was immobilized via *N*-ethyl-*N*′-(3-dimethylaminopropyl) carbodiimide and *N*-hydroxysuccinimide. Storage at 4 ºC gave this biosensor a shelf life of about 12 weeks. Similarly, a PANI/carboxymethyl cellulose (CMC) nanocomposite deposited on ITO coated glass using glutaraldehyde as cross-linker showed a shelf life of 10 weeks when stored at 4 ºC [163].

Saini et al. [164] reported a bienzymatic cholesterol biosensor based on PANI/Au/graphene nanocomposite. Both ChOx and horseradish peroxidase (HRP) were immobilized on the surface of the nanocomposite. Studies reveal that this bienzyme immobilized bioelectrode

[2] Micromolar

facilitates efficient electron transfer between the bienzyme and the electrode, thereby exhibiting better performance over monoenzymatic biosensor.

3.2.1.3. Peroxide biosensors

Hydrogen peroxide (H_2O_2) is a byproduct of a wide range of biological processes, and plays an important role in various cellular activities of mammalian cells [165-167]. H_2O_2 has also been found to be toxic to cells - together with the superoxide anion and the hydroxyl radical it forms the reactive oxygen species in the body, which is capable of causing macromolecular damage to cells [168]. Due to its varying cellular functions, detection and quantification of H_2O_2 is necessary to understand the underlying mechanism in its production and function. Generally, horseradish peroxidase (HRP) is employed for peroxide detection. HRP immobilized on PANI/polyester sulphonic acid (PESA) nanocomposite has been reported to detect H_2O_2 with a detection limit of 0.185 μM [169]. A PANI/chitosan nanocomposite film with HRP immobilized on its surface was used by Du et al. [170] for H_2O_2 detection. While the enzyme catalyzed the reduction of H_2O_2, the nanocomposite enabled rapid electron transfer between the active centers of the enzyme and electrode.

3.2.1.4. Other enzymatic biosensors

Several other enzymes have been immobilized on PANI nanocomposites enabling detection of an array of compounds. One of these is uricase which is used for sensing uric acid. Devi and Pundir [171] reported a covalently immobilized uricase on Fe_3O_4/chitosan/PANI nanocomposite electrode. The hybrid composition of the electrode facilitated charge transfer resulting in a appreciable sensitivity of 0.44 mA mM^{-1} at a detection limit of 0.1 μM in under 1s. A nanocomposite of Prussian blue nanoparticles, carboxylated MWCNTs (cMWCNTs) and PANI has also exhibited good sensitivity towards uric acid [172]. The enzyme uricase

was immobilized onto the nanocomposite surface via chitosan-glutaraldehyde cross-linking. Similarly, creatinine can also be detected using enzyme immobilized PANI nanocomposites. PANI/cMWCNTs with enzymes creatinine amidohydrolase, creatine amidinohydrolase, and sarcosine oxidase immobilized onto it via *N*-ethyl-*N*′-(3-dimethylaminopropyl) carbodiimide and *N*-hydroxy succinimide has shown promising results [173]. This tri-enzyme system was also utilized by Yadav et al. [174] for creatinine detection wherein the enzymes were immobilized on Fe_3O_4/chitosan/PANI nanocomposite electrode which gave a fast response with a detection limit of 1 μM.

Very recently, Zhybak and coworkers [175] demonstrated a creatinine deaminase and urease immobilized ammonium ion-specific Cu/PANI nanocomposite for creatinine and urea detection. The biosensors were characterized by high selectivity, sensitivity and fast response. Figure 15 shows the amperometric response of creatinine and urea biosensors. The addition of glucose induced prevented loss of enzyme activity providing better homogeneity to the biosensor membrane. The creatinine and urea sensors exhibited excellent sensitivity of ~ 95 and 91 mA M^{-1} cm^{-2}.

3.2.2. Immunosensors

The combination of antigen-antibody specificity and transducer forms the basis of an immunosensor. Huang et al. [176] described a multicomponent system for detection of salbutamol. They prepared a nanocomposite of PANI with Au nanoparticles, Prussian blue, poly(acrylic acid) and Au-graphene. A label of chitosan coated graphene with nano-Au shell was attached to immobilize HRP-anti-SAL antibody on this multicomponent nanocomposite. The immunosensor showed good catalytic activity for hydrogen reduction on the electrode. Liu and coworkers [177] prepared GO/PANI/CdSe nanocomposite for detection of interleukin-6. The electrochemiluminescence of CdSe was greatly improved by combining

with graphene oxide/PANI. The nanocomposite showed high specificity, long term stability and reproducibility with detection limit as low as 0.17 pg/mL[3].

PANI/Au nanocomposite has been used for detection of prostate-specific antigen (PSA) [178]. The sensor performance was measured using differential pulse voltammetry (DPV) which studied the electrochemical changes resulting from the biochemical reactions on the surface. The nanocomposite provided a high surface area for immobilization of anti-PSA, and resulted in increased electron transfer which improved the performance of the immunosensor. Figure 16 shows the electrochemical response studies of the immunosensor to different concentrations of PSA. The sensor exhibited good linearity, high sensitivity and excellent response at very low concentrations. The immunosensor showed stability for up to 5 weeks after which a decrease in response current was observed.

A multilayer nanocomposite of Au/PANI/cMWCNTs/chitosan has been used for detection of chlorpyrifos, an organophosphate insecticide [179]. The Au nanoparticle on the surface of the nanocomposite provided an excellent platform for immobilization of anti-chlorpyrifos antibody. The immunosensor showed superior sensitivity and specific immunoreactions even when used for analysis of real samples. Like other biosensors, storage at low temperatures affords the sensor a longer shelf life. Detection of estradiol by graphene/PANI nanocomposite based immunosensor has been reported by Li et al. [180]. Carboxylated graphene oxide was used as the carrier for HRP-antibody immobilization on the sensor surface, which improved the catalytic activity of the hydrogen reduction of electrode. The immunosensor showed a wide range of linearity with a low detection limit of 0.02 ng/mL[4]. Lin et al. [181] reported the detection of benzo[a]pyrene (BaP) using a multi-enzyme antibody of HRP-HCS-secondary antibody immobilized on Fe_3O_4/PANI/Nafion sensor. The nanocomposite provided an efficient electron transfer pathway for reduction of H_2O_2.

[3] Picogram/milliliter
[4] Nanogram/milliliter

A label-free immunosensor has been developed by Yan et al. [182] for detection of low density lipoproteins (LDL). Apolipoprotein B-100 antibody was immobilized on the surface of Au-AgCl/PANI nanocomposite, and the sensor performance was measured by electrochemical impedance spectroscopy (EIS). Label-free biosensors enable monitoring of real time biochemical reactions while providing a scope for exploring modulation factors. The poor conductivity of LDL and the negative charges carried by it brings about a change in electron transfer resistance which enabled its detection. The immunosensor gave a very low detection limit of 0.34 pg/mL at an optimized incubation time of 50 min and incubation temperature of 37 ºC. PANI based hybrid materials provide an efficient transducer to which the immunochemical reactions can be coupled. The ease of fabrication and tunability of PANI properties by combination of nanomaterials allows facile label-free detection of antigens.

3.2.3. DNA biosensors

Biosensors aimed at DNA detection are so fabricated as to provide high sensitivity and accurate and rapid detection. The development of DNA biosensors stems from its applicability in the fields of forensics, gene analysis, biological warfare detection and DNA diagnostics [145]. A single-stranded DNA (ssDNA) probe immobilized on the transducer surface recognizes its complementary DNA target by hybridization. Wu and coworkers [183] reported a PANI/graphite oxide nanocomposite over carbon paste electrode (CPE) for monitoring DNA hybridization. Their results indicated that both ssDNA and dsDNA (double-strand DNA) change the redox characteristics of the nanocomposite electrode. Square wave voltammetry (SWV), used to monitor hybridization and detect the complementary ssDNA, revealed good stability and reproducibility for the sensor, and showed that its responses were influenced by factors like pH and incubation time. Other researchers [184,185] too used

nanocomposites of graphene and PANI for DNA sensing. Wang and coworkers [186] designed a layered biosensor by fabricating graphene sheets on GCE followed by electropolymerization of PANI and electro-deposition of Au nanoparticles for detection of BCR/ABL fusion gene in chronic myelogenous leukemia (CML). The ssDNA probe was dually labeled at 5′ and 3′ with -SH and biotin, respectively. Following hybridization, the 3′-biotin site face moved away from the electrode surface, binding the streptavidin-alkaline phosphatase. The hydrolysis of 1-naphthyl phosphate to 1-naphthol was monitored via DPV. The biosensor showed high selectivity with a detection limit of 2.11 pM[5].

A label-free electrochemical DNA sensor based on PPY/PANI/Au nanocomposite used ssDNA labeled with 6-mercapto-1-hexane for hybridization [187]. The biopolymer enhanced the hybridization efficiency of the ssDNA as compared to the lone Au nanoparticle based transducer. The biosensor was highly sensitive towards the complementary ssDNA with a low detection limit of 10^{-13} M. Forster and coworkers [188,189] employed a PANI nanocomposite with surface deposited Au nanoparticles as DNA biosensor. In one of their reports [188], thiolated ssDNA, which is complementary to a sequence of *Stephylococcus aureus*, was immobilized onto the nanocomposite surface. HRP labeled probe strand was hybridized to an unbound section of the capture strand. Target concentration was quantified by current measurements during reduction of benzoquinone through HRP.

Yang et al. [190] reported a PANI/MWCNT nanocomposite for detection of phosphinothricin acetyltransferase gene (PAT), which is one of the screening detection genes for the transgenic plants. An ssDNA probe was immobilized onto the nanocomposite and hybridization was detected through EIS. The authors conducted the test on a real sample of genetically modified soybean. PAT has also been detected using PANI/ZrO_2 nanocomposites with polytyrosine [191]. The nanocomposite aided in ssDNA immobilization and hybridization, which were

[5] Picomolar

studied by CV and EIS. The electron transfer resistance was found to increase with concentration of target DNA. It should however be noted that both these nanocomposites, i.e., PANI/MWCNT and PANI/ZrO_2, exhibited the same detection limit. Another study reports the detection of DNA base (guanine, adenine, thymine, and cytosine) using PANI/MnO_2 nanocomposite [192]. Radhakrishnan et al. [193] described a PPY/PANI nanocomposite with ssDNA immobilized onto it via glutarladehyde, and using methyl blue as electrochemical indicator. The biosensor exhibited a high sensitivity with a detection limit of 50 fM^6. DNA biosensors have also been employed for pesticide detection. For example, a nucleic acid based biosensor for pesticide detection has been reported by Prahakar et al. [194]. The *calf thymus* dsDNA immobilized on PANI/polyvinyl sulphonate (PVS) nanocomposite exhibited high stability for up to 6 months. In DNA biosensors, the immobilization of nucleic acid probe sequence onto a transducer while maintaining its activity is crucial to the device's performance. Hybridization with the target DNA changes the doping level of PANI, and therefore its conductivity.

4. Conclusion and Future Challenges

PANI nanocomposites has shown much promise as a sensing element, as reflected by its multitude of applications. However, their commercialization still remains a challenge for scientists across the world due to the fact that PANI itself suffers from a number of drawbacks. First of them is regarding the synthesis of PANI. To avoid secondary growth and retain its nanostructure, controlled synthesis of PANI at optimized pH and temperature is necessary. Dopant also plays a very important role in formation of PANI, as well as its electronic properties. Depending on the type of dopant, PANI can be highly conducting, self-doped, and/or soluble in water or different organic solvents. PANI in doped form can have a

[6] Femtomolar

relatively short shelf life. A secondary component in PANI can have a synergistic effect in improving its shelf life in doped form, and various other properties, and thus applicability. Hence, fabrication of PANI nanocomposites with an extended life in doped form is essential for its long service life.

Nanocomposites of PANI show better properties as compared to neat PANI. However, in many cases the secondary component also tends to reduce its electrical conductivity. Nevertheless, PANI nanocomposites offer safer detection of number combustible and toxic gases at room temperature by inducing selectivity and higher sensitivity into the material. Room temperature sensing not only prevents response variation resulting from structural changes in the sensing material at high temperatures, but also avoids sensor instability thus extending its shelf life. However, the sensor response of a large number of these nanocomposites is influenced by humidity which may cause false responses in the material. Hence, developing PANI nanocomposites impervious to humidity is one of the great challenges. An increased electron transfer capability of PANI nanocomposites is also desirable for detection of biological agents. Immobilization of biological agents onto PANI transducers becomes more feasible when a secondary component has been combined with PANI. A better interaction between the components of the nanocomposite will enhance the efficiency and performance of the sensor manifold.

Finally, new strategies need to be devised in order to fully understand the underlying mechanism involved in analyte sensing by PANI and its nanocomposites, which will enable us in fabrication and commercialization of highly selective sensors for specific agents.

Acknowledgements

One of the authors (T. Sen) is thankful to the University Grants Commission, New Delhi, India for providing financial support under the Non-SAP RFSMS scheme.

References

[1] M. Wan, Conducting polymers with micro or nanometer structure, Tsinghua University Press, Beijing and Springer-Verlag GmbH, Berlin, Heidelberg, 2008, pp. 3.

[2] G.G. Wallace, G.M. Spinks, L.A.P. Kane-Maguire, P.R. Teasdale, Conductive electroactive polymers, Taylor & Francis Group, LLC, Florida, 2009, pp. 137.

[3] N. Gospodinova, L. Terlemezyan, Conducting polymers prepared by oxidative polymerization: polyaniline, Prog. Polym. Sci. 23 (1998) 1443–1484.

[4] X. Lua, W. Zhanga, C. Wanga, T.-C. Wenb, Y. Wei, One-dimensional conducting polymer nanocomposites: Synthesis, properties and applications, Prog. Polym. Sci. 36 (2011) 671–712.

[5] E.T. Kang, K.G. Neoha, K.L. Tan, Polyaniline: A Polymer with Many Interesting Intrinsic Redox States, Prog. Polym. Sci., 23 (1998) 277-324.

[6] Y.-Z. Longa, M.-M. Li, C. Gub, M. Wan, J.-L. Duvaild, Z. Liue, Z. Fan, Recent advances in synthesis, physical properties and applications of conducting polymer nanotubes and nanofibers, Prog. Polym. Sci. 36 (2011) 1415– 1442.

[7] A. Rahy, D.J. Yang, Synthesis of highly conductive polyaniline nanofibers, Mater. Lett. 62 (2008) 4311–4314.

[8] Z.J. Gu, J.R. Ye, W. Song, Q. Shen, Synthesis of polyaniline nanotubes with controlled rectangular or square pore shape, Mater. Lett. 121 (2014) 12–14.

[9] M. Ayad, G. El-Hefnawy, S. Zaghlol, Facile synthesis of polyaniline nanoparticles; its adsorption behavior, Chemical Engineering Journal 217 (2013) 460–465.

[10] Y.F. Kuang, C.P. Fu, H.H. Zhu, Polyaniline Nanocomposites, in: S. Thomas, G.E. Zaikov, (Eds.), Polymer Nanocomposite Research Advances, Nova Science, New York, 2008, pp. 314.

[11] J. Jang , J. Ha, K. Kim, Organic light-emitting diode with polyaniline-poly(styrene sulfonate) as a hole injection layer, Thin Solid Films 516 (2008) 3152–3156.

[12] Z. Zhou, X. Zhang, C. Lu, L. Lan, G. Yuan, Polyaniline-decorated cellulose aerogel nanocomposite with strong interfacial adhesion and enhanced photocatalytic activity, RSC Adv. 4 (2014) 8966-8972.

[13] A.A. Khan, L. Paquiza, Characterization and ion-exchange behavior of thermally stable nano-composite polyaniline zirconium titanium phosphate: Its analytical application in separation of toxic metals, Desalination, 265 (2011) 242-254.

[14] P. Bober, J. Stejskal, M. Trchova, J. Prokes, In-situ prepared polyaniline–silver composites: Single- and two-step strategies, Electrochim. Acta (2013) http://dx.doi.org/10.1016/j.electacta.2013.10.001.

[15] L. Li, G. Yan, J. Wu, X. Yu, Q. Guo, Preparation of polyaniline-metal composite nanospheres by in situ microemulsion polymerization, J. Colloid Interface Sci. 326 (2008) 72-75.

[16] P. Boomi, H.G. Prabu, Synthesis, characterization and antibacterial analysis of polyaniline/Au–Pd nanocomposite, Colloids Surf., A 429 (2013) 51-59.

[17] P. Boomi, H.G. Prabu, J. Mathiyarasu, Synthesis and characterization of polyaniline/Ag–Pt nanocomposite for improved antibacterial activity. Colloids Surf., B 103 (2013) 9-14.

[18] H. Guleryuz, C. Filiatre, M. Euvrard, C. Buron, B. Lakard, Novel strategy to prepare polyaniline-Modified SiO_2/TiO_2 composite particles, Synth. Met. 181 (2013) 104-109.

[19] Q. Xiao, X. Tan, L. Ji, J. Xue, Preparation and characterization of polyaniline/nano-Fe_3O_4 composites via a novel Pickering emulsion route, Synth. Met. 157 (2007) 784-791.

[20] F. Huang, E. Vanhaecke, D. Chen, In situ polymerization and characterizations of polyaniline on MWCNT powders and aligned MWCNT films, Catal. Today 150 (2010) 71-76.
[21] O.-K. Park, T. Jeevananda, N.H. Kim, S.-il Kim, J.H. Lee, Effects of surface modification on the dispersion and electrical conductivity of carbon nanotube/polyaniline composites, Scr. Mater. 60 (2009) 551-554.
[22] Y.-C. Lin, F.-H. Hsu, T.-M. Wu, Enhanced conductivity and thermal stability of conductive polyaniline/graphene composite synthesized by in situ chemical oxidation polymerization with sodium dodecyl sulfate, Synth. Met. 184 (2013) 29-34.
[23] Q. Zhang, Y. Li, Y. Feng, W. Feng, Electropolymerization of graphene oxide/polyaniline composite for high-performance supercapacitor, Electrochim. Acta 90 (2013) 95-100.
[24] S.V. Bhat, S.R.C. Vivekchand, Optical spectroscopic studies of composites of conducting PANI with CdSe and ZnO nanocrystals, Chem. Phys. Lett. 433 (2006) 154-158.
[25] S. Zhang, Q. Chen, D. Jing, Y. Wang, L. Guo, Visible photoactivity and antiphotocorrosion performance of PdS–CdS photocatalysts modified by polyaniline, Int. J. Hydrogen Energy 37 (2012) 791-796.
[26] B.H.F. Moura, R.H.B. Assis, P.I.B.M. Franco, N.R. Antoniosi Filho, D. Rabelo, Synthesis and characterization of composites based on polyaniline and styrene-divinylbenzene copolymer using benzoyl peroxide as oxidant agent. React. Funct. Polym. 73 (2013) 1255-1261.
[27] Z. Ben Othmen, A. Fattoum, M. Arous, Dielectric study of polyaniline/poly (methylmethacrylate) composite films below the percolation threshold, J. Electrostat. 71 (2013) 999-1004.
[28] D.N. Huyen, Carbon Nanotubes and Semiconducting Polymer Nanocomposites, in: Carbon Nanotubes - Synthesis, Characterization, Applications, S. Yellampalli (Ed.), In Tech, Croatia, 2011, pp. 469-486.
[29] K. Gupta, P.C. Jana, A.K. Meikap, Optical and Electrical Transport Properties of Polyaniline-Silver Nano-composite, Synth. Met. 160 (2010) 1566–1573.
[30] Z.-A. Hu, Y.-L. Xie, Y.-X. Wang, L.-P. Mo, Y.-Y. Yang, Z.-Y. Zhang, Polyaniline/SnO_2 nanocomposite for supercapacitor applications, Mater. Chem. Phys. 114 (2009) 990-995.
[31] A. Olad, R. Nosrati, Preparation, characterization, and photocatalytic activity of polyaniline/ZnO nanocomposite, Res. Chem. Intermed. 38 (2012) 323–336.
[32] P. Kannusamy, T. Sivalingam, Chitosan–ZnO/polyaniline hybrid composites: Polymerization of aniline with chitosan–ZnO for better thermal and electrical property, Polym. Degrad. Stab. 98 (2013) 988-996.
[33] G. Qiu, Q. Wang, M. Nie, Polyaniline/Fe_3O_4 magnetic nanocomposite prepared by ultrasonic irradiation, J. Appl. Polym. Sci. 102 (2006) 2107–2111.
[34] M.D. Bedre, S. Basavaraja, B.D. Salwe, V. Shivakumar, L. Arunkumar, A. Venkataraman, Preparation and characterization of Pani and Pani-Ag nanocomposites via interfacial polymerization, Polym. Compos. 30 (2009) 1668-1677.
[35] B. Zhang, B. Zhao, S. Huang, R. Zhang, P. Xu, H.-L. Wang, One-pot interfacial synthesis of Au nanoparticles and Au–polyaniline nanocomposites for catalytic applications, Cryst. Eng. Comm. 14 (2012) 1542.
[36] F.-J. Liu, L.-M. Huang, T.-C. Wen, A. Gopalan, J.-S. Hung, Interfacial synthesis of platinum loaded polyaniline nanowires in poly(styrene sulfonic acid), Mater. Lett. 61 (2007) 4400-4405.

[37] V. Divya, M.V. Sangaranarayanan, A facile synthetic strategy for mesoporous crystalline copper- polyaniline nanocomposites, Eur. Polym. J. 48 (2012) 560–568.
[38] W. Cho, S.-J. Park, S. Kim, Effect of monomer concentration on interfacial synthesis of platinum loaded polyaniline nanocomplex using poly(styrene sulfonic acid), Synth. Met. 161 (2011) 2446-2450.
[39] J.M. Kinyanjui, N.R. Wijeratne, J. Hanks, D.W. Hatchett, Chemical and electrochemical synthesis of polyaniline/platinum composites, Electrochim. Acta 51 (2006) 2825-2835.
[40] S. Jing, S. Xing, L. Yu, Y. Wu, C. Zhao, Synthesis and Characterization of Ag/polyaniline core-shell nanocomposites based on silver nanoparticles colloids, Mater. Lett. 61 (2007) 2794–2797.
[41] S.S. Barkade, J.B. Naik, S.H. Sonawane, Ultrasound assisted miniemulsion synthesis of polyaniline/Ag nanocomposite and its application for ethanol vapor sensing. Colloids Surf., A 378 (2011) 94-98.
[42] S. Mishra, N.G. Shimpi, T. Sen, The effect of PEG encapsulated silver nanoparticles on the thermal and electrical property of sonochemically synthesized polyaniline/silver nanocomposite, J. Polym. Res. 20 (2013) 49-58.
[43] A. Houdayer, R. Schneider, D. Billaud, J. Ghanbaja, J. Lambert, New polyaniline/Ni(0) nanocomposites: Synthesis, charac terization and evaluation of their catalytic activity in Heck couplings, Synth. Met. 151 (2005) 165-174.
[44] M.G. Hosseini, S. Zeynali, M.M. Momeni, R. Najjar, Polyaniline nanofibers supported on titanium as templates for immobilization of Pd nanoparticles: A new electro-catalyst for hydrazine oxidation, J. Appl. Polym. Sci. 124 (2012) 4671–4677.
[45] L. Kong, X. Lu, E. Jin, S. Jiang, C. Wang, W. Zhang, Templated synthesis of polyaniline nanotubes with Pd nanoparticles attached onto their inner walls and its catalytic activity on the reduction of p-nitroanilinum, Compos. Sci. Technol. 69 (2009) 561–566.
[46] K. Basavaiah, Y. Pavan Kumar, A.V. Prasada Rao, A facile one-pot synthesis of polyaniline/magnetite nanocomposites by micelles-assisted method, Appl. Nanosci. 3 (2013) 409–415.
[47] S. Zhu, W. Wei, X. Chen, M. Jiang, Z. Zhou, Hybrid structure of polyaniline/ZnO nanograss and its application in dye-sensitized solar cell with performance improvement. J. Solid State Chem. 190 (2012) 174-179.
[48] B. Wang, C. Liu, Y. Yin, S. Yu, K. Chen, P. Liu, B. Liang, Double template assisting synthesized core–shell structured titania/polyaniline nanocomposite and its smart electrorheological response, Compos. Sci. Technol. 86 (2013) 89-100.
[49] Z. Wang, H. Bi, J. Liu, T. Sun, X. Wu, Magnetic and microwave absorbing properties of polyaniline/γ-Fe_2O_3 nanocomposite, J. Magn. Mag. Mater. 320 (2008) 2132-2139.
[50] S. Sathiyanarayanan, S.S. Azim, G. Venkatachari, Preparation of polyaniline–Fe_2O_3 composite and its anticorrosion performance, Synth. Met. 157 (2007) 751-757.
[51] A. Mostafaei, A. Zolriasatein, Synthesis and characterization of conducting polyaniline nanocomposites containing ZnO nanorods, Prog. Nat. Sci. 22 (2012) 273-280.
[52] B.I. Nandapure, S.B. Kondawar, M.Y. Salunkhe, A.I. Nandapure, Magnetic and Transport Properties of Conducting polyaniline/nickel Oxide Nanocomposites, Adv. Mat. Lett. 4 (2013) 134-140.
[53] M.D. Bedre, R. Deshpande, B. Salimath, V. Abbaraju, Preparation and Characterization of Polyaniline-Co_3O_4 Nanocomposites via Interfacial Polymerization, Am. J. Mater. Sci. 2 (2012) 39-43.
[54] T. Sen, N.G. Shimpi, S. Mishra, R.P. Sharma, Polyaniline/γ-Fe_2O_3 nanocomposite for room temperature LPG sensing, Sens. Actuators, B. 190 (2014) 120-126.

[55] G. Li, C. Zhang, H. Peng, K. Chen. One-dimensional V_2O_5@polyaniline core/shell nanobelts synthesized by an in situ polymerization method. Macromol. Rapid. Commun. 30 (2009) 1841–5.
[56] S. Pang, G. Li, Z. Zhang, Synthesis of Polyaniline-Vanadium Oxide Nanocomposite Nanosheets, Macromol. Rapid. Commun. 26 (2005) 1262-1265.
[57] C.R.K. Rao, M. Vijayan, Ruthenium(II)-mediated synthesis of conducting polyaniline (PAni): A novel route for PAni–RuO_2 composite, Synth. Met. 158 (2008) 516-519.
[58] S.L. Patil, S.G. Pawar, M.A. Chougule, B.T. Raut, P.R. Godse, S. Sen; V.B. Patil, Structural, Morphological, Optical, and Electrical Properties of PANi-ZnO Nanocomposites, Int. J. Polym. Mater. Polym. Biomater. 61 (2012) 809-820.
[59] S.L. Patil, M.A. Chougule, S.G. Pawar, S. Sen, A.V. Moholkar, J.H. Kim, V.B. Patil, Fabrication of Polyaniline-ZnO Nanocomposite Gas Sensor, Sens. Transducers J. 134 (2011) 120-131.
[60] X. Zhang, J. Zhang, R. Wang, Z. Liu. Cationic surfactant directed polyaniline/CNT nanocables: synthesis, characterization, and enhanced electrical properties, Carbon 42 (2004) 1455-1461.
[61] A. Vega-Rios, F.Y. Renteria-Baltierrez, C.A. Hernandez-Escobar, E.A. Zaragoza-Contreras, A new route toward graphene nanosheet/polyaniline composites using a reactive surfactant as polyaniline precursor, Synth. Met. 184 (2013) 52-60.
[62] S. Srivastava, S.S. Sharma, S. Agrawal, S. Kumar, M. Singh, Y.K. Vijay, Study of chemiresistor type CNT doped polyaniline gas sensor, Synth. Met. 160 (2010) 529-534.
[63] C. Oueiny, S. Berlioz, F.-X. Perrin, Carbon nanotube–polyaniline composites, Prog. Polym. Sci. (2013) http://dx.doi.org/10.1016/j.progpolymsci.2013.08.009.
[64] F. Huang, E. Vanhaecke, D. Chen, In situ polymerization and characterizations of polyaniline on MWCNT powders and aligned MWCNT films, Catal. Today 150 (2010) 71-76.
[65] Q. Jiang, G. Fu, D. Xie, S. Jiang, Z. Chen, B. Huang, Y. Zhao, Preparation of carbon nanotube/polyaniline nanofiber by electrospinning, Procedia Eng. 27 (2012) 72-76.
[66] M. Hezarjaribi, M. Jahanshahi, A. Rahimpour, M. Yaldagard, Gas diffusion electrode based on electrospun Pani/CNF nanofibers hybrid for proton exchange membrane fuel cells (PEMFC) applications, Appl. Surf. Sci. 295 (2014) 144-149.
[67] M.K. Shin, Y.J. Kim, S.I. Kim, S.-K. Kim, H.Lee, G.M. Spinks, S.J. Kim, Enhanced conductivity of aligned PANi/PEO/MWNT nanofibers by Electrospinning, Sens. Actuators, B 134 (2008) 122–126.
[68] P. Kar, A. Choudhury, Carboxylic acid functionalized multi-walled carbon nanotube doped polyaniline for chloroform sensors, Sens. Actuators, B 183 (2013) 25-33.
[69] M. Kumar, K. Singh, S.K. Dhawan, K. Tharanikkarasu, J.S. Chung, B.-S. Kong, E.J. Kim, S.H. Hur, Synthesis and characterization of covalently-grafted graphene–polyaniline nanocomposites and its use in a supercapacitor, Chem. Eng. J. 231 (2013) 397-405.
[70] J. Luo, S. Jiang, R. Liu, Y. Zhang, X. Liu, Synthesis of water dispersible polyaniline/poly(styrenesulfonic acid) modified graphene composite and its electrochemical properties, Electrochim. Acta 96 (2013) 103-109.
[71] Y. Li, H. Peng, G. Li, K. Chen, Synthesis and electrochemical performance of sandwich-like polyaniline/graphene composite nanosheets, Eur. Polym. J. 48 (2012) 1406-1412.
[72] Y.F. Huang, C.W. Lin, Facile synthesis and morphology control of graphene oxide/polyaniline nanocomposites via in-situ polymerization process, Polymer 53 (2012) 2574-2582.

[73] R. Li, L. Liu, F. Yang, Preparation of polyaniline/reduced graphene oxide nanocomposite and its application in adsorption of aqueous Hg(II), Chem. Eng. J. 229 (2013) 460-468.
[74] S. Ameen, M.S. Akhtar, Y.S. Kim, H.S. Shin, Synthesis and electrochemical impedance properties of CdS nanoparticles decorated polyaniline nanorods, Chem. Eng. J. 181–182 (2012) 806-812.
[75] B.T. Raut, P.R. Godse, S.G. Pawar, M.A. Chougule, D.K. Bandgar, S. Sen, V.B. Patil. New process for fabrication of polyaniline–CdS nanocomposites: Structural, morphological and optoelectronic investigations, J. Phys. Chem. Solids 74 (2013) 236-244.
[76] E. Tuncer, E. Turac, Synthesis and Characterization of Polyaniline/Zinc Sulfite Composite Films and Investigation of Properties, Adv. Polym. Tech. 32 (2013) DOI: 10.1002/adv.21373.
[77] H. Zhuang, J.-B. Liu, Q.-H. Zeng, X.-G. Kong, Effect of Polyaniline as Hole-Acceptor and Energy-Acceptor on the Photoluminescence of CdSe, Chem. Res. Chin. Univ. 23 (2007) 131-134.
[78] Y. Haldorai, V.H. Nguyen, J.-J. Shim, Synthesis of polyaniline/Q-CdSe composite via ultrasonically assisted dynamic inverse emulsion polymerization, Colloid. Polym. Sci. 289 (2011) 849–854.
[79] V. Zucolotto, M. Ferreira, M.R. Cordeiro, C.J.L. Constantino, W.C. Moreira, O.N. Oliveira Jr., Nanoscale processing of polyaniline and phthalocyanines for sensing applications, Sens. Actuators B 113 (2006) 809-815.
[80] J.C.B. Santos, L.G. Paterno, E.A.T. Dirani, F.J. Fonseca, A.M. de Andrade, Influence of polyaniline and phthalocyanine hole-transport layers on the electrical performance of light-emitting diodes using MEH-PPV as emissive material, Thin Solid Films 516 (2008) 3184-3188.
[81] X. Lu, D. Shan, J. Yang, B. Huang, X. Zhou, Determination of m-dinitrobenzene based on novel type of sensor using thiol-porphyrin mixed monolayer-tethered polyaniline with intercalating fullerenols, Talanta 115 (2013) 457-461.
[82] Q. Zhou, C. Li, J. Li, J. Lu, Electrocatalysis of template electrosynthesized cobalt-porphyrin/polyaniline nanocomposite for oxygen reduction, J. Phys. Chem. C 112 (2008) 18578–18583.
[83] S. Adhikari, P. Banerji, Polyaniline composite by in situ polymerization on a swollen PVA gel, Synth. Met. 159 (2009) 2519-2524.
[84] A.K. Bajpai, J. Bajpai, S.N. Soni, Designing Polyaniline (PANI) and Polyvinyl Alcohol (PVA) Based Electrically Conductive Nanocomposites: Preparation, Characterization and Blood Compatible Study, J. Macromol. Sci., Pure Appl. Chem. 46 (2009) 774–782.
[85] M.C. Arenas, G. Sanchez, O. Martinez-Alvarez, V.M. Castano, Electrical and morphological properties of polyaniline–polyvinyl alcohol in situ nanocomposites, Composites Part B 56 (2014) 857-861.
[86] D.S. Patil, J.S. Shaikh, D.S. Dalavi, S.S. Kalagi, P.S. Patil, Chemical synthesis of highly stable PVA/PANI films for supercapacitor application, Mater. Chem. Phys. 128 (2011) 449-455.
[87] P.L.B. Araujo, E.S. Araujo, R.F.S. Santos, A.P.L. Pacheco, Synthesis and morphological characterization of PMMA/polyaniline nanofiber composites, Microelectron. J. 36 (2005) 1055-1057.
[88] G. Panthi, N.A. Barakat, A.M. Hamza, A.R. Unnithan, M. Motlak, K.A. Khalil, Y.-S. Shin, H.Y. Kim, Polyaniline-Poly(vinyl acetate) Electrospun Nanofiber Mats as Novel Organic Semiconductor Material, Sci. Adv. Mater. 4 (2012) 1118-1126(9).

[89] J.B. Veluru, K.K. Satheesh, D.C. Trivedi, V.R. Murthy, N.T. Srinivasan, Electrical properties of electrospun fibers of PANI-PMMA composites, J. Eng. Fibers Fabr. 2 (2007) 25-31.
[90] X. Lu, H. Dou, S. Yang, L. Hao, L. Zhang, L. Shen, F. Zhang, X. Zhang, Fabrication and electrochemical capacitance of hierarchical graphene/polyaniline/carbon nanotube ternary composite film, Electrochim. Acta 56 (2011) 9224-9232.
[91] Q. Cheng, J. Tang, N. Shinya, L.-C. Qin, Polyaniline modified graphene and carbon nanotube composite electrode for asymmetric supercapacitors of high energy density, J. Power Sources 241 (2013) 423-428.
[92] J. Yan, T. Wei, Z. Fan, W. Qian, M. Zhang, X. Shen, F. Wei, Preparation of graphene nanosheet/carbon nanotube/polyaniline composite as electrode material for supercapacitors, J. Power Sources 195 (2010) 3041-3045.
[93] Z.-D. Huang, R. Liang, B. Zhang, Y.-B. He, J.-K. Kim, Evolution of flexible 3D graphene oxide/carbon nanotube/polyaniline composite papers and their supercapacitive performance, Compos. Sci. Technol. 88 (2013) 126-133.
[94] S. Wang, H. Bao, P. Yang, G. Chen, Immobilization of trypsin in polyaniline-coated nano-Fe_3O_4/carbon nanotube composite for protein digestion, Anal. Chim. Acta 612 (2008) 182-189.
[95] N.G. Shimpi, D.P. Hansora, R. Yadava, S. Mishra, Performance of hybrid nanostructured conductive cotton threads as LPG sensor at ambient temperature: preparation and analysis, RSC Adv. 5 (2015) 99253-99269.
[96] J. Zhao, Y. Xie, C. Yu, Z. Le, R. Zhong, Y. Qin, J. Pan, F. Liu, Preparation and characterization of the graphene–carbon nanotube/$CoFe_2O_4$/polyaniline composite with reticular branch structures, Mater. Chem. Phys. 142 (2013) 395-402.
[97] X.-W. Hu, C.-J. Mao, J.-M. Song, H.-L. Niu, S.-Y. Zhang, H.-P. Huang. Fabrication of GO/PANi/CdSe nanocomposites for sensitive electrochemiluminescence biosensor, Biosens. Bioelectron. 41 (2013) 372-378.
[98] H. Xu, X. Chen, J. Zhang, J. Wang, B. Cao, D. Cui, NO_2 gas sensing with SnO2–ZnO/PANI composite thick film fabricated from porous nanosolid, Sens. Actuators, B 176 (2013) 166-173.
[99] P. Boomi, H.G. Prabu, Synthesis, characterization and antibacterial analysis of polyaniline/Au–Pd nanocomposite, Colloids Surf., A 429 (2013) 51-59.
[100] P. Boomi, H.G. Prabu, J. Mathiyarasu, Synthesis and characterization of polyaniline/Ag–Pt nanocomposite for improved antibacterial activity. Colloids Surf., B 103 (2013) 9-14.
[101] P. Boomi, H.G. Prabu, J. Mathiyarasu, Synthesis, characterization and antibacterial activity of polyaniline/Pt–Pd nanocomposite, Eur. J. Med. Chem. 72 (2014) 18-25.
[102] Q. Yu, M. Shi, Y. Cheng, M. Wang, H.-Z. Chen, Fe_3O_4@Au/polyaniline multifunctional nanocomposites: their preparation and optical, electrical and magnetic properties, Nanotechnology 19 (2008) 265702, DOI: 10.1088/0957-4484/19/26/265702.
[103] Y. Lee, E. Kim, K. Kim, B.H. Lee, S. Choe, Polyaniline effect on the conductivity of the PMMA/Ag hybrid composite, Colloids Surf., A 396 (2012) 195–202.
[104] C.-Y. Li, W.-Y. Chiu, T.-M. Don, Polyurethane/Polyaniline and Polyurethane-Poly(methylmethacrylate)/Polyaniline Conductive Core-Shell Particles: Preparation, Morphology, and Conductivity, J. Polym. Sci., Part A: Polym. Chem. 45 (2007) 3902–3911.
[105] T. Jeevananda, Siddaramaiah, Synthesis and characterization of polyaniline filled PU/PMMA interpenetrating polymer networks, Eur. Polym. J. 39 (2003) 569–578.
[106] J. Janata, Principles of Chemical Sensors, fourth ed., Springer, New York, 2009.

[107] H. Bai, G. Shi, Gas Sensors Based on Conducting Polymers, Sensors 7 (2007) 267-307.
[108] A.A. Athawale, S.V. Bhagwat, P.P. Katre, Nanocomposite of Pd-polyaniline as a selective methanol sensor, Sens. Actuators, B. 114 (2006) 263-267.
[109] A. Choudhury, Polyaniline/silver nanocomposites. Dielectric properties and ethanol vapour sensitivity. Sens. Actuators, B 138 (2009) 318-325.
[110] Z.-F. Li, F.D. Blum, M.F. Bertino, C.-S. Kim, Understanding the response of nanostructured polyaniline gas sensors, Sens. Actuators, B 183 (2013) 419-427.
[111] S. Sharma, C. Nirkhe, S. Pethkar, A.A. Athawale, Chloroform vapour sensor based on copper/polyaniline nanocomposite, Sens. Actuators, B. 85 (2002) 131-136.
[112] S.G. Pawar, S.L. Patil, M.A. Chougule, P.R. Godse, D.K. Bandgar, V.B. Patil, Fabrication of Polyaniline/TiO2 Nanocomposite Ammonia Vapor Sensor, J. Nano-Electron. Phys. 3 (2011) 1056-1063.
[113] M. Dhingra, L. Kumar, S. Shrivastava, P. Senthil Kumar, S. Annapoorni, Impact of interfacial interactions on optical and ammonia sensing in zinc oxide/polyaniline nanostructures, Bull. Mater. Sci. 36 (2013) 647–652.
[114] N.G. Deshpande, Y.G. Gudage, R.P. Sharma, J.C. Vyas, J.B. Kim, Y.P. Lee, Studies on tin oxide-intercalated polyaniline nanocomposite for ammonia gas sensing applications, Sens. Actuators, B. 138 (2009) 76–84.
[115] G.D. Khuspe, S.T. Navale, M.A. Chougule, V.B. Patil, Ammonia gas sensing properties of CSA doped PANi-SnO_2 nanohybrid thin films, Synth. Met. 185–186 (2013) 1–8.
[116] H.-D. Zhang, C.-C. Tang, Y.-Z. Long, J.-C. Zhang, R. Huanga, J.-J. Li, C.-Z. Gu, High-sensitivity gas sensors based on arranged polyaniline/PMMAcomposite fibers, Sens. Actuators, A 219 (2014) 123–127.
[117] L. Zhihua, Z. Xucheng, S. Jiyong, Z. Xiaobo, H. Xiaowei, H.E. Tahir, M. Holmes, Fast response ammonia sensor based on porous thin film of polyaniline/sulfonated nickel phthalocyanine composites, Sens. Actuators, B 226 (2016) 553–562.
[118] K. Crowley, A. Morrin, R.L. Shepherd, M. in het Panhuis, G.G. Wallace, M.R. Smyth, A.J. Killard, Fabrication of Polyaniline-Based Gas Sensors Using Piezoelectric Inkjet and Screen Printing for the Detection of Hydrogen Sulfide, IEEE Sens. J. 10 (2010) 1419-1426.
[119] J. Sarfraz, P. Ihalainen, A. Määttänen, J. Peltonen, M. Lindén, Printed hydrogen sulfide gas sensor on paper substrate based on polyaniline composite, Thin Solid Films 534 (2013) 621–628.
[120] B.T. Raut, P.R. Godse, S.G. Pawar, M.A. Chougule, D.K. Bandgar, V.B. Patil, Novel method for fabrication of polyaniline–CdS sensor for H_2S gas detection, Measurement 45 (2012) 94–100.
[121] M.D. Shirsat, M.A. Bangar, M.A. Deshusses, N.V. Myung, A. Mulchandani, Polyaniline nanowires-gold nanoparticles hybrid network based chemiresistive hydrogen sulfide sensor, Appl. Phys. Lett. 94 (2009) 083502-083504.
[122] S.S. Joshi, C.D. Lokhande, S.-H. Han, A room temperature liquefied petroleum gas sensor based on all-electrodeposited n-CdSe/p-polyaniline junction, Sens. Actuators, B. 123 (2007) 240–245.
[123] D.S. Dhawale, R.R. Salunkhe, U.M. Patil, K.V. Gurav, A.M. More, C.D. Lokhande, Room temperature liquefied petroleum gas (LPG) sensor based on p-polyaniline/n-TiO_2 heterojunction, Sens. Actuators, B 134 (2008) 988–992.
[124] D.S. Dhawale, D.P. Dubal, V.S. Jamadade, R.R. Salunkhe, S.S. Joshi, C.D. Lokhande, Room temperature LPG sensor based on n-CdS/p-polyaniline heterojunction, Sens. Actuators, B 145 (2010) 205–210.

[125] D.S. Dhawale, D.P. Dubal, A.M. More, T.P. Gujar, C.D. Lokhande, Room temperature liquefied petroleum gas (LPG) sensor, Sens. Actuators, B. 147 (2010) 488–494.
[126] S.K. Shukla, Vamakshi, Minakshi, A. Bharadavaja, A. Shekhar, A. Tiwari, Fabrication of electro-chemical humidity sensor based on zinc oxide/polyaniline nanocomposites, Adv. Mat. Lett. 3(5) (2012) 421-425.
[127] A. Vijayan, M. Fuke, R. Hawaldar, M. Kulkarni, D. Amalnerkar, R.C. Aiyer, Optical fibre based humidity sensor using Co-polyaniline clad, Sens. Actuators, B. 129 (2008) 106-112.
[128] M.V. Fuke, P. Kanitkar, M. Kulkarni, B.B. Kale, R.C. Aiyer, Effect of particle size variation of Ag nanoparticles in Polyaniline composite on humidity sensing, Talanta 81 (2010) 320-326.
[129] N. Parvatikar, S. Jain, S. Khasim, M. Revansiddappa, S.V. Bhoraskar, M.V.N. Ambika Prasad, Electrical and humidity sensing properties of polyaniline/WO_3 composites, Sens. Actuators, B. 114 (2006) 599-603.
[130] K.C. Sajjan, M. Faisal, S.C. Vijaya Kumari, Y.T. Ravikiran, S. Khasim, Proceeding of International Conference on Recent Trends in Applied Physics and Material Science: RAM 2013. AIP Conference Proceedings, 1536 (2013) 289-290. DOI: 10.1063/1.4810214.
[131] R.S. Diggikar, M.V. Kulkarni, G.M. Kale, B.B. Kale, Formation of multifunctional nanocomposites with ultrathin layers of polyaniline (PANI) on silver vanadium oxide (SVO) nanospheres by in situ polymerization. J. Mater. Chem. A 1 (2013) 3992-4001.
[132] P. Cavallo, D. Acevedo, M.C. Fuertes, G.J.A.A Soler-Illia, C. Barbero, Understanding the sensing mechanism of polyaniline resistive sensors. Effect of humidity on sensing of organic volatiles, Sens. Actuators, B 210 (2015) 574-580.
[133] X. Yan, G. Xie, X. Du, H. Tai, Y. Jiang, Preparation and characterization of polyaniline/indium(III) oxide (PANi/In_2O_3) nanocomposite thin film, Proc. SPIE 7282, 4th International Symposium on Advanced Optical Manufacturing and Testing Technologies: Advanced Optical Manufacturing Technologies, 72823C (May 21, 2009); doi:10.1117/12.831026.
[134] M.K. Ram, O. Yavuz, V. Lahsangah, M. Aldissi, CO gas sensing from ultrathin nanocomposite conducting polymer film, Sens. Actuators, B. 106 (2005) 750-757.
[135] I. Kim, K.-Y. Dong, B.-K. Ju, H.H. Choi, Gas sensor for CO and NH_3 using polyaniline/CNTs composite at room temperature, Nanotechnology (IEEE-NANO), 2010 10th IEEE Conference, Seoul (2010) 466 – 469, DOI 10.1109/NANO.2010.5697782.
[136] J. Yun, S. Jeon, H.-I. Kim, Improvement of NO Gas Sensing Properties of Polyaniline/MWCNT Composite by Photocatalytic Effect of TiO_2, Journal of Nanomaterials 2013 (2013), Article ID 184345, http://dx.doi.org/10.1155/2013/184345.
[137] H. Xu, X. Chen, J. Zhang, J. Wang, B. Cao, D. Cui, NO_2 gas sensing with SnO_2–ZnO/PANI composite thick film fabricated from porous nanosolid, Sens. Actuators, B. 176 (2013) 166-173.
[138] S. Srivastava, S. Kumar, S. Agrawal, A. Saxena, B.L. Choudhary, S. Mathur, M. Singh, Y.K. Vijay, TiO_2/PANI and MWNT/PANI Composites Thin Films for Hydrogen Gas Sensing, International Conference on Physics of Emerging Functional Materials (PEFM-2010), Mumbai, India, 1313 (2010), ISBN: 978-0-7354-0868-5, D.K. Aswal, A.K. Debnath, eds.
[139] R. Arsat, X. He, P. Spizzirri, M. Shafiei, M. Arsat, W. Wlodarski, Hydrogen Gas Sensor Based on Highly Ordered Polyaniline/Multiwall Carbon Nanotubes Composite, Sensor Lett. 9(2) (2011) 940-943.

[140] A. Sadek, W. Wlodarski, K. Shin, R. Kaner, K. Kalantar-Zadeh, A polyaniline/WO_3 nanofiber composite-based ZnO/64° YX LiNbO(3)SAW hydrogen gas sensor, Synth. Met. 158 (2008) 29-32.
[141] C. Conn, S. Sestak, A.T. Baker, J. Unsworth, A Polyaniline-Based Selective Hydrogen Sensor. Electroanalysis 10(16) (1998) 1137-1141.
[142] M.E. Azim-Araghi, M.J. Jafari, Electrical and gas sensing properties of polyaniline-chloroaluminium phthalocyanine composite thin films, Eur. Phys. J. Appl. Phys. 52 (2010) 10402-10407.
[143] S.J. Updike, G.P. Hicks, The Enzyme Electrode, Nature 214 (1976) 986-988.
[144] A.A. Karyakin, Biosensors, in: M.I. Baraton (Ed.), Sensors for Environment, Health and Security, Springer, The Netherlands, 2009, pp. 255-262.
[145] C. Dhanda, M. Dasa, M. Datta, B.D. Malhotra, Recent advances in polyaniline based biosensors, Biosens. Bioelectron. 26 (2011) 2811–2821.
[146] D. Wei, A. Ivaska, Electrochemical Biosensors Based on Polyaniline, Chem. Anal. (Warsaw) 51 (2006) 839-852.
[147] M.D. Imisides, R. John, G.G. Wallace, Microsensors based on conducting polymers, Chemtech 261 (1996) 9-25.
[148] Z. Muhammad-Tahir, E.C. Alocilja, A conductometric biosensor for biosecurity, Biosens. Bioelectron. 18 (2003) 813.
[149] A. Malinauskas, R. Garjonyte, R. Mazeikiene, I. Jureviciute, Electrochemical response of ascorbic acid at conducting and electrogenerated polymer modified electrodes for electroanalytical applications: a review, Talanta 64 (20040 121-129.
[150] D.T. Hoa, T.N. Suresh Kunar, N.S. Punekar, R.S. Srinivasa, R. Lal, A.Q. Contractor, A biosensor based on conducting polymers, Anal. Chem. 64 (1992) 2645-2646.
[151] L.C. Clark, C. Lyons, Electrode systems for continuous monitoring in cardiovascular surgery, Ann. N. Y. Acad. Sci. 102 (1962) 29-45.
[152] Y. Xian, Y. Hu, F. Liu, Y. Xiang, H. Wang, L. Jin, Glucose baiosensor based on Au nanoparticles-conductive polyaniline nanocomposite, Biosens. Bioelectron. 21 (2006) 1996-2000.
[153] Q. Xu, S.-X. Gu, L. Jin, Y.-e Zhou, Z. Yang, W. Wang, X. Hu, Graphene/polyaniline/gold nanoparticles nanocomposite for the direct electron transfer of glucose oxidase and glucose biosensing, Sens. Actuators, B. 190 (2014) 562–569.
[154] A.I. Gopalan, K.P. Lee, D. Ragupathy, S.H. Lee, J.W. Lee, An electrochemical glucose biosensor exploiting a polyaniline grafted multiwalled carbon nanotube/ perfluorosulfonate ionomer–silica nanocomposite, Biomaterials 30 (2009) 5999-6005.
[155] H. Zhong, R. Yuan, Y. Chai, W. Li, X. Zhong, Y. Zhang, In situ chemo-synthesized multi-wall carbon nanotube-conductive polyaniline nanocomposites: characterization and application for a glucose amperometric biosensor, Talanta 85(1) (2011) 104-111.
[156] T.H. Le, N.T. Trinh, L.H. Nguyen, H.B. Nguyen, V.A. Nguyen, D.L. Tran, T.D. Nguyen, Electrosynthesis of polyaniline–mutilwalled carbon nanotubes nanocomposite films in the presence of sodium dodecyl sulfate for glucose biosensing, Adv. Nat. Sci.: Nanosci. Nanotechnol. 4 (2013) 025014, DOI 10.1088/2043-6262/4/2/025014.
[157] J. Zhu, X. Liu, X. Wang, X. Huo, R. Yan, Preparation of polyaniline-TiO_2 nanotube composite for the development of electrochemical biosensors, Sens. Actuators, B 221 (2015) 450-457.
[158] C. Ozdemir, F. Yeni, D. Odaci, S. Timur, Electrochemical glucose biosensing by pyranose oxidase immobilized in gold nanoparticle-polyaniline/AgCl/gelatin nanocomposite matrix, Food Chemistry 119 (2010) 380-385.

[159] M. Srivastava, S.K Srivastava, N.R. Nirala, R. Prakash, Chitosan-based Polyaniline-Au Nanocomposite Biosensor for Determination of Cholesterol, Anal. Methods (2013) Accepted Manuscript, DOI: 10.1039/C3AY41812J.
[160] N. Ruecha, R. Rangkupan, N. Rodthongkum, O. Chailapakul, Novel paper-based cholesterol biosensor using graphene/polyvinylpyrrolidone/polyaniline nanocomposite, Biosens.Bioelectron. 52 (2014) 13-19.
[161] R.K. Basniwal, R.P. Singh Chauhan, S. Parvez, V.K. Jain, Development of a Cholesterol Biosensor by Chronoamperometric Deposition of Polyaniline-Ag Nanocomposites, International Journal of Polymeric Materials and Polymeric Biomaterials 62 (2013) 493-498.
[162] C. Dhand, S.K. Arya, M. Datta, B.D. Malhotra, Polyaniline–carbon nanotube composite film for cholesterol biosensor, Anal. Biochem. 383 (2008) 194-199.
[163] A. Barik, P.R. Solanki, A. Kaushik, A. Ali, M.K. Pandey, C.G. Kim, B.D. Malhotra, Polyaniline-Carboxymethyl Cellulose Nanocomposite for Cholesterol Detection, J. Nanosci. Nanotechnol. 10 (2010) 6479-6488.
[164] D. Saini, R. Chauhan, P.R. Solanki, T. Basu, Gold-Nanoparticle Decorated Graphene-Nanostructured Polyaniline Nanocomposite-Based Bienzymatic Platform for Cholesterol Sensing, ISRN Nanotechnology (2012) DOI:10.5402/2012/102543.
[165] B. D'Autreaux, M.B. Toledano, ROS as signaling molecules: mechanisms that generate specificity in ROS homeostasis, Nat. Rev. Mol. Cell Biol. 8 (2007) 813-824.
[166] M. Giorgio, M. Trinei, E. Migliaccio, P.G. Pelicci, Hydrogen peroxide: a metabolic by-product or a common mediator of ageing signals? Nat. Rev. Mol. Cell Biol. 8 (2007) 722-728.
[167] S.G. Rhee, Cell signaling. H_2O_2, a necessary evil for cell signaling, Science 312 (2006) 1882-1883.
[168] S.G. Rhee, T.-S. Chang, W. Jeong, D. Kang, Methods for Detection and Measurement of Hydrogen Peroxide Inside and Outside of Cells, Mol. Cells 29 (2010) 539-549.
[169] A. Al-Ahmed, P.M. Ndangili, N. Jahed, P.G.L. Baker, E.I. Iwuoha, Polyester Sulphonic Acid Interstitial Nanocomposite Platform for Peroxide Biosensor, Sensors (Basel) 9(12) (2009) 9965–9976.
[170] Z. Du, C. Li, L. Li, M. Zhang, S. Xu, T. Wang, Simple fabrication of a sensitive hydrogen peroxide biosensor using enzymes immobilized in processable polyaniline nanofibers/chitosan film, Mater. Sci. Eng., C 29 (2009) 1794-1797.
[171] R. Devi, C.S. Pundir, Construction and application of an amperometric uric acid biosensor based on covalent immobilization of uricase on iron oxide nanoparticles/chitosan-g-polyaniline composite film electrodeposited on Pt electrode, Sens. Actuators, B. 193 (2014) 608-615.
[172] R. Rawal, S. Chawla, N. Chauhan, T. Dahiya, C.S. Pundir. Construction of amperometric uric acid biosensor based on uricase immobilized on PBNPs/cMWCNT/PANI/Au composite, Int. J. Biol. Macromol. 50(1) 2012 112-118.
[173] S. Yadav, A. Kumar, C.S. Pundir, Amperometric creatinine biosensor based on covalently coimmobilized enzymes onto carboxylated multiwalled carbon nanotubes/polyaniline composite film, Anal. Biochem.419 (2011) 277-283.
[174] S. Yadav, R. Devi, P. Bhar, S. Singhla, C.S. Pundir, Immobilization of creatininase, creatinase and sarcosine oxidase on iron oxide nanoparticles/chitosan-g-polyaniline modified Pt electrode for detection of creatinine, Enzyme Microb. Technol. 50 (2012) 247-254.
[175] M. Zhybak, V. Beni, M.Y. Vagin, E. Dempsey, A.P.F. Turner, Y. Korpan, Creatinine and urea biosensors based on a novel ammonium ion-selective copper-polyaniline nano-composite, Biosens. Bioelectron. 77 (2016) 505-511.

[176] J. Huang, Q. Lin, X. Zhang, X. He, X. Xing, W. Lian, M. Zuo, Q. Zhang, Electrochemical immunosensor based on polyaniline/poly (acrylic acid) and Au-hybrid graphene nanocomposite for sensitivity enhanced detection of salbutamol, Food Res. Int. 44 (2011) 92-97.
[177] P.-Z. Liu, X.-W. Hu, C.-J. Mao, H.-L. Niu, J.-M. Song, B.-K. Jin, S.-Y. Zhang, Electrochemiluminescence immunosensor based on graphene oxide nanosheets/polyaniline nanowires/CdSe quantum dots nanocomposites for ultrasensitive determination of human interleukin-6, Electrochim. Acta 113 (2013) 176-180.
[178] A. Dey, A. Kaushik, S.K. Arya, S. Bhansali, Mediator free highly sensitive polyaniline–gold hybrid nanocomposite based immunosensor for prostate-specific antigen (PSA) detection, J. Mater. Chem. 22 (2012) 14763-14772.
[179] X. Sun, L. Qiao, X. Wang, A Novel Immunosensor Based on Au Nanoparticles and Polyaniline/Multiwall Carbon Nanotubes/Chitosan Nanocomposite Film Functionalized Interface, Nano-Micro Letters 5(3) 2013 191-201.
[180] J. Li, S. Liu, J. Yu, W. Lian, M. Cui, W. Xu, J. Huang, Electrochemical immunosensor based on graphene–polyaniline composites and carboxylated graphene oxide for estradiol detection, Sens. Actuators, B. 188 (2013) 99-105.
[181] M. Lin, Y. Liu, Z. Sun, S. Zhang, Z. Yang, C. Ni, Electrochemical immunoassay of benzo[a]pyrene based on dual amplification strategy of electron-accelerated Fe_3O_4/polyaniline platform and multi-enzyme-functionalized carbon sphere label, Anal. Chim. Acta 722 (2012) 100-106.
[182] W. Yan, X. Chen, X. Li, X. Feng, J.-J. Zhu, Fabrication of a Label-Free Electrochemical Immunosensor of Low-Density Lipoprotein, J. Phys. Chem. B 112 (2008) 1275-1281.
[183] J. Wu, Y. Zou, X. Li, H. Liu, G. Shen, R. Yu, A biosensor monitoring DNA hybridization based on polyaniline intercalated graphite oxide nanocomposite, Sens. Actuators, B. 104 (2005) 43-49.
[184] Y. Bo, H. Yang, Y. Hu, T. Yao, S. Huang, A novel electrochemical DNA biosensor based on graphene and polyaniline nanowires, Electrochim. Acta 56 (2011) 2676-2681.
[185] M. Du, T. Yang, X. Li, K. Jiao, Fabrication of DNA/graphene/polyaniline nanocomplex for label-free voltammetric detection of DNA hybridization, Talanta 88 (2012) 439-444.
[186] L. Wang, E. Hua, M. Liang, C. Ma, Z. Liu, S. Sheng, M. Liu, G. Xie, W. Feng, Graphene sheets, polyaniline and AuNPs based DNA sensor for electrochemical determination of BCR/ABL fusion gene with functional hairpin probe, Biosens. Bioelectron. 51 (2014) 201-207.
[187] J. Wilson, S. Radhakrishnan, C. Sumathi, V. Dharuman, Polypyrrole–polyaniline–Au (PPy–PANi–Au) nano composite films for label-free electrochemical DNA sensing, Sens. Actuators, B. 171-172 (2012) 216–222.
[188] E. Spain, T.E. Keyes, R.J. Forster, Vapour phase polymerised polyaniline–gold nanoparticle composites for DNA detection, J. Electroanal. Chem. 711 (2013) 38-44.
[189] E. Spain, R. Kojima, R.B. Kaner, G.G. Wallace, J. O'Grady, K. Lacey, T. Barry, T.E. Keyes, R.J. Forster, High sensitivity DNA detection using gold nanoparticle functionalised polyaniline nanofibers, Biosens. Bioelectron. 26 (2011) 2613-2618.
[190] T. Yang, N. Zhou, Y. Zhang, W. Zhang, K. Jiao, G. Li, Synergistically improved sensitivity for the detection of specific DNA sequences using polyaniline nanofibers and multi-walled carbon nanotubes composites, Biosens. Bioelectron. 24 (2009) 2165-2170.
[191] J. Yang, X. Wang, H. Shi, An electrochemical DNA biosensor for highly sensitive detection of phosphinothricin acetyltransferase gene sequence based on polyaniline-(mesoporous nanozirconia)/poly-tyrosine film, Sens. Actuators, B. 162 (2012) 178-183.

[192] M.U. Anu Prathap, R. Srivastava, B. Satpati, Simultaneous detection of guanine, adenine, thymine, and cytosine at polyaniline/MnO_2 modified electrode, Electrochimica Acta 114 (2013) 285-295.
[193] S. Radhakrishnan, C. Sumathi, V. Dharuman, J. Wilson, Polypyrrole nanotubes–polyaniline composite for DNA detection using methylene blue as intercalator, Anal. Methods 5 (2013) 1010-1015.
[194] N. Prabhakar, G. Sumana, K. Arora, H. Singh, B.D. Malhotra, Improved electrochemical nucleic acid biosensor based on polyaniline-polyvinyl sulphonate, Electrochim. Acta 53 (2008) 4344-4350.

Captions to figures

Figure 1. Molecular structures of typical intrinsically conducting polymers.

Figure 2. TEM micrograph showing uniformly dispersed Ag nanoparticles in PANI matrix.

Figure 3. SEM images of Pd-NPs deposited on the PANI film with different magnifications (a,b) [44]. (Copyright © 2012 by John Wiley & Sons, Inc. This material is reproduced with permission of John Wiley & Sons, Inc.)

Figure 4. (a) The schematic procedure of PANI hybridizing ZnO nanograss, (b) side view FE-SEM images of ZnO nanograss obtained by hydrothermal methods, and (c) hybridized sample with 100 mg/L PANI. The insert images show top views. (Reprinted with permission [47])

Figure 5. FE-SEM micrographs of (a) γ-Fe_2O_3 nanoparticles (500 nm) and PANi/γ-Fe_2O_3 nanocomposites at 1 wt% (b), 2 wt% (c) and 3 wt% (d) (1μm). (Reprinted with permission [54])

Figure 6. SEM (a) and (b) and dark field TEM (c) and (d) images of pristine MWCNT (inset), carboxyl-functionalized MWCNT and 2 wt% MWCNT-contained PANI/c MWCNT nanocomposite. (Reprinted with permission [68])

Figure 7. SEM images of PANI/CNT (a), PANI/CNT-2 (b) and PANI (c); TEM images of GO–PANI/CNT (d) and GO–PANI (e). (Reprinted with permission [90])

Figure 8. General response curve of a sensor [106]. (Reproduced from Principles of Chemical Sensors, 2009, page 4, Introduction to Sensors, Jiri Janata, with kind permission of Springer Science+Business Media.)

Figure 9. I–V curves (in the presence of ammonia gas) for (a) tin oxide, (b) polyaniline and (c) tin oxide/polyaniline nanocomposites. (Reprinted with permission [114])

Figure 10. (a) Response and recovery transients (solid line) of gold nanoparticles functionalized PANI nanowire network based chemiresistive sensor toward 0.1 ppb, 1 ppb, 10 ppb, 100 ppb, 500 ppb, and 1 ppm (dashed line) concentrations of H_2S gas, (b) Response of unfunctionalized PANI nanowire network toward 50 ppm of H_2S gas (—— indicates carrier gas and ←→ indicates gas analyte) [121]. Reproduced with permission from [M.D. Shirsat, M.A. Bangar, M.A. Deshusses, N.V. Myung, A. Mulchandani, Polyaniline nanowires-gold nanoparticles hybrid network based chemiresistive hydrogen sulfide sensor, Appl. Phys. Lett. 94 (2009) 083502-083504]. Copyright [2009], AIP Publishing LLC.

Figure 11. Current-voltage (I-V) curve of PANi/γ-Fe_2O_3 nanocomposite at 3 wt% γ-Fe_2O_3 content (F3) in air and at different LPG concentrations. (Reprinted with permission [54])

Figure 12. NO gas sensing behaviour of various samples under UV irradiation. (Reprinted with permission from [136])

Figure 13. Schematic representation of biosensor operation.

Figure 14. Amperometric response of GOx/PANi–MWCNT/IDμE upon increasing the glucose concentration in steps of 1mM at +0.6V (versus SCE) in PBS. Inset shows the calibration plot [156]. (Reproduced with permission from IOPscience)

Figure 15. (A) An example of the amperometric response of the creatinine biosensor to successive additions of creatinine (-0.35 V, PBS pH 7.4). (B) An example of the amperometric response of the urea biosensor to successive additions of urea (-0.35 V, PBS pH 7.4). (C) Calibration curve for creatinine, urea and ammonium ion detection obtained at creatinine and urea biosensors and PANi-Nafion-Cu-modified SPE. (Reprinted with permission [175])

Figure 16. (A) Electrochemical response studies of the BSA/anti-PSA/ AuNP–PSA/Au immunoelectrode as a function of PSA (1 pg mL^{-1} to 100 ng mL^{-1}) in PBS (10 mM, pH 7 containing 0.9% NaCl) using DPV technique. Inset (a) calibration curve between magnitude of electrochemical response current vs. logarithm of PSA concentration and inset (b) shelf-life studies of BSA/anti-PSA/AuNP–PSA/Au immunoelectrode. (B) Interference studies of BSA/anti-PSA/AuNP–PSA/Au immunoelectrode using BSA (10 ng mL^{-1}) and cortisol (10 ng mL^{-1}) with respect to PSA (10 ng mL^{-1}). Reproduced from [178] with permission from The Royal Society of Chemistry.

Biographies

Tanushree Sen obtained her M.Sc. in 2006 in Polymer Science. She is presently pursuing Ph.D. from University Institute of Chemical Technology, North Maharashtra University, Jalgaon, Maharashtra, India. Her areas of research are intrinsically conducting polymers, nanocomposites, gas sensors, fiber reinforced plastics, and polymeric blends and alloys.

Navinchandra G. Shimpi completed his Ph.D. in 2006. He is presently Associate Professor at the Department of Chemistry, University of Mumbai. He has 37 published research papers in various international and national journals. He has a research experience of 10 years on areas such as polymer nano composites, rubber composites and nano-fillers.

Satyendra Mishra did his Ph.D. from Indian Institute of Technology, Delhi in 1989. He is presently the Director of University Institute of Chemical Technology, North Maharashtra University, Jalgaon, Maharashtra. He has been continually engaged in research activities for the last 30 years. He has over 140 published research papers in various international and national journals. His areas of research are polymer nano composites, water soluble polymers, wood polymer composites, nano-polymers, reaction engineering aspects of depolymerization reactions, nano catalysis and gas sensors.

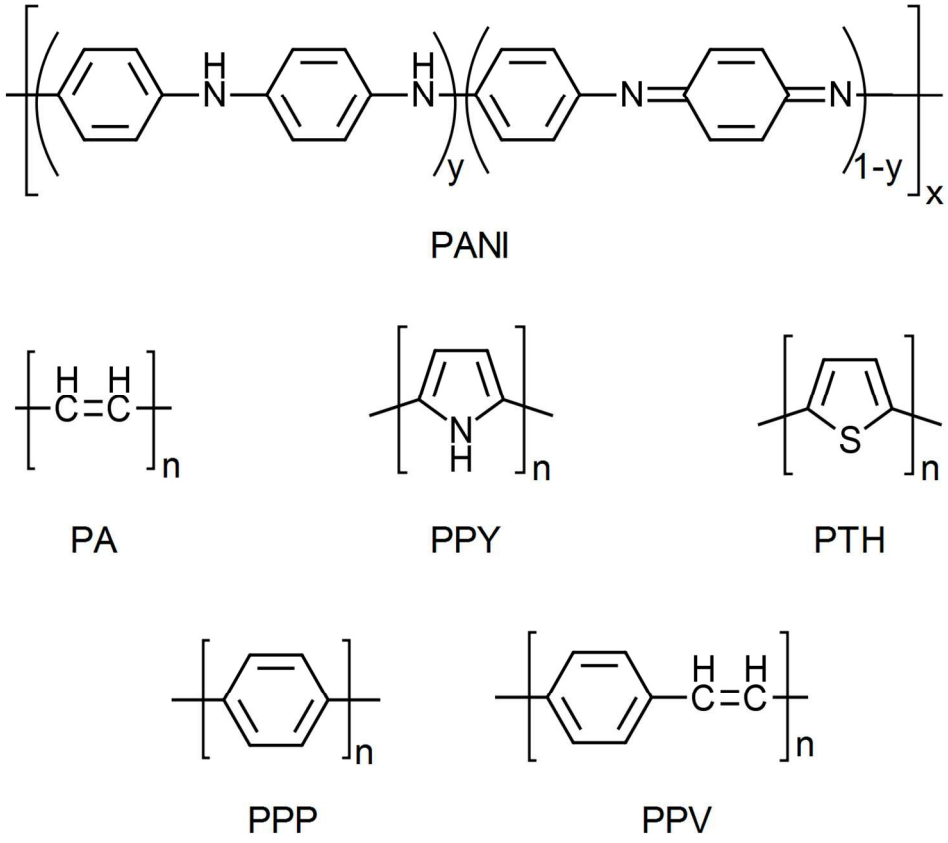

Figure 1. Molecular structures of typical intrinsically conducting polymers.
541x482mm (72 x 72 DPI)

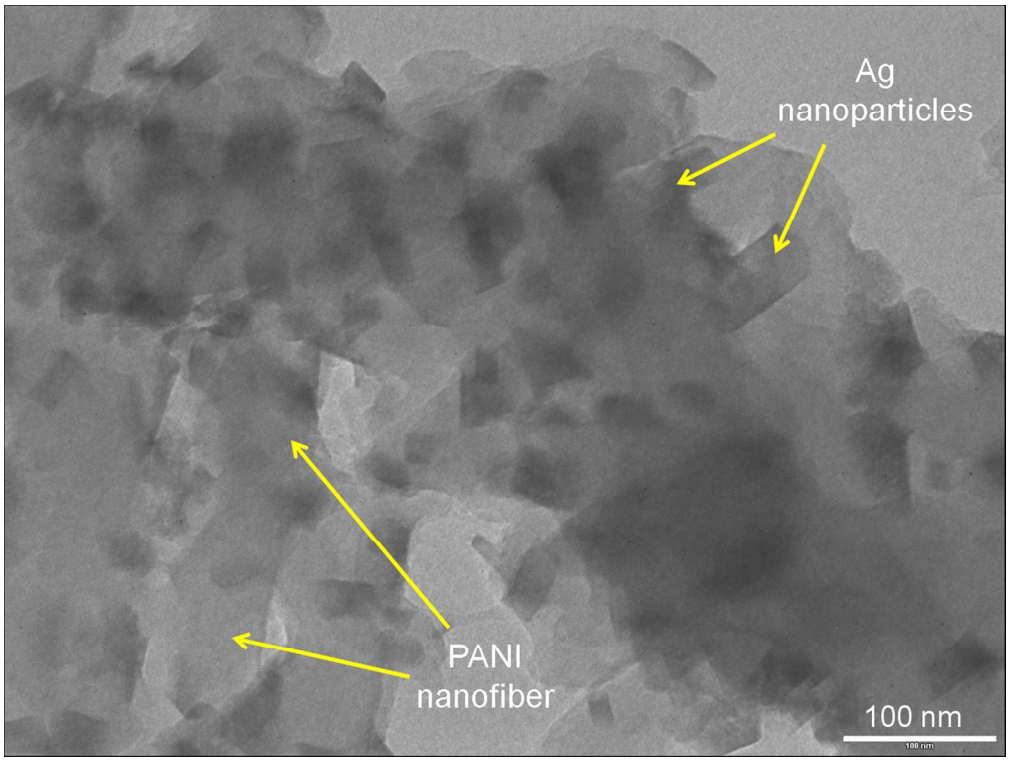

Figure 2. TEM micrograph showing uniformly dispersed Ag nanoparticles in PANI matrix.
214x161mm (150 x 150 DPI)

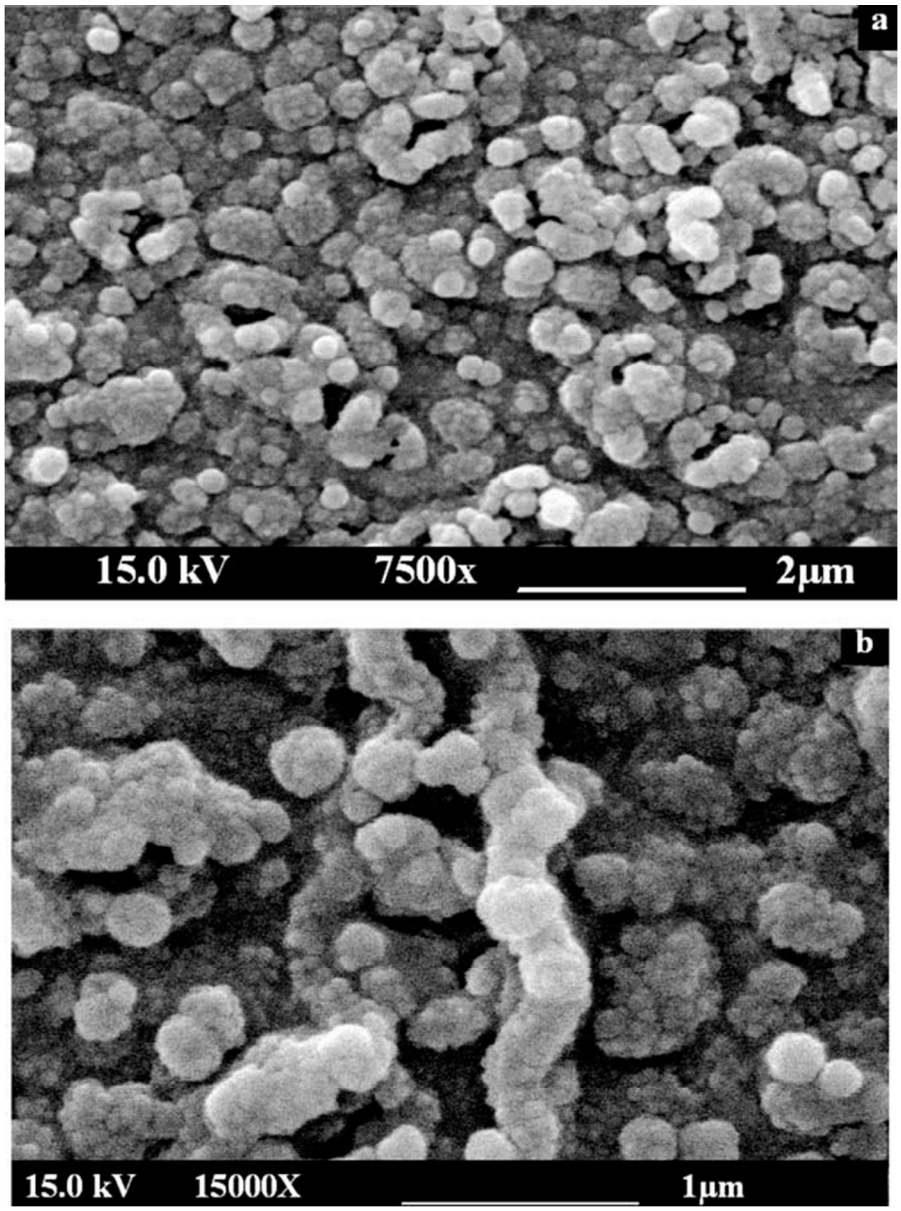

Figure 3. SEM images of Pd-NPs deposited on the PANI film with different magnifications (a,b) [44].

172x232mm (96 x 96 DPI)

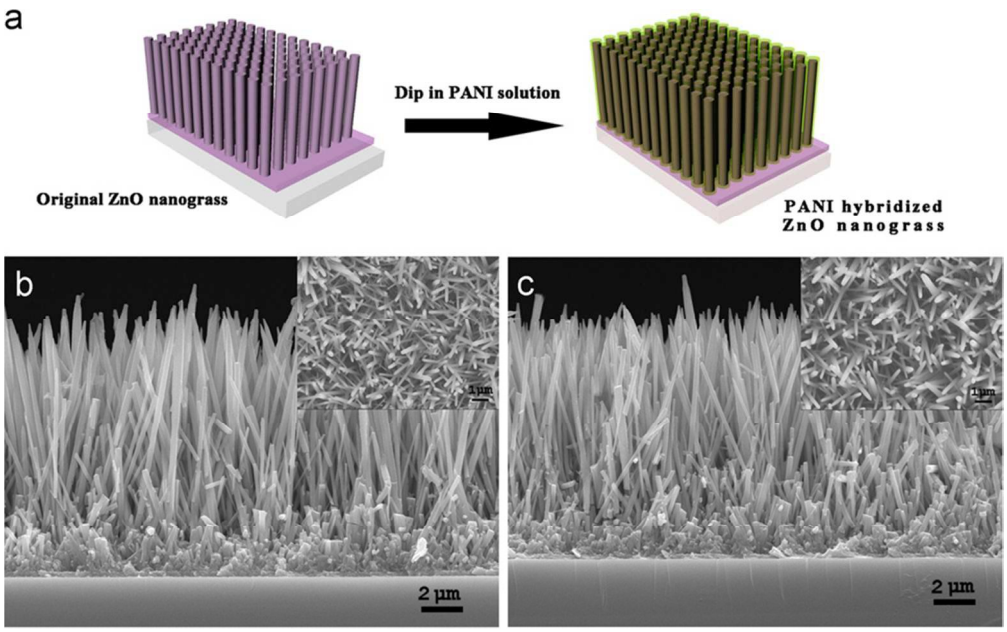

Figure 4. (a) The schematic procedure of PANI hybridizing ZnO nanograss, (b) side view FE-SEM images of ZnO nanograss obtained by hydrothermal methods, and (c) hybridized sample with 100 mg/L PANI. The insert images show top views. (Reprinted with permission [47])
254x157mm (96 x 96 DPI)

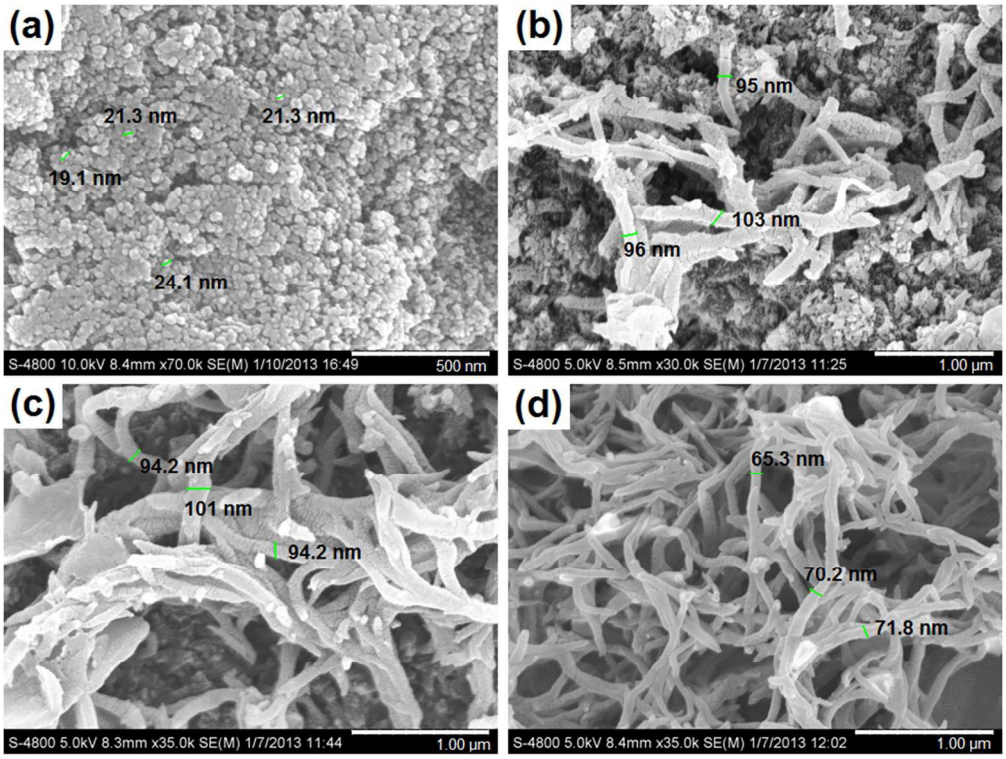

Figure 5. FE-SEM micrographs of (a) γ-Fe2O3 nanoparticles (500 nm) and PANi/γ-Fe2O3 nanocomposites at 1 wt% (b), 2 wt% (c) and 3 wt% (d) (1µm). (Reprinted with permission [54])
257x193mm (96 x 96 DPI)

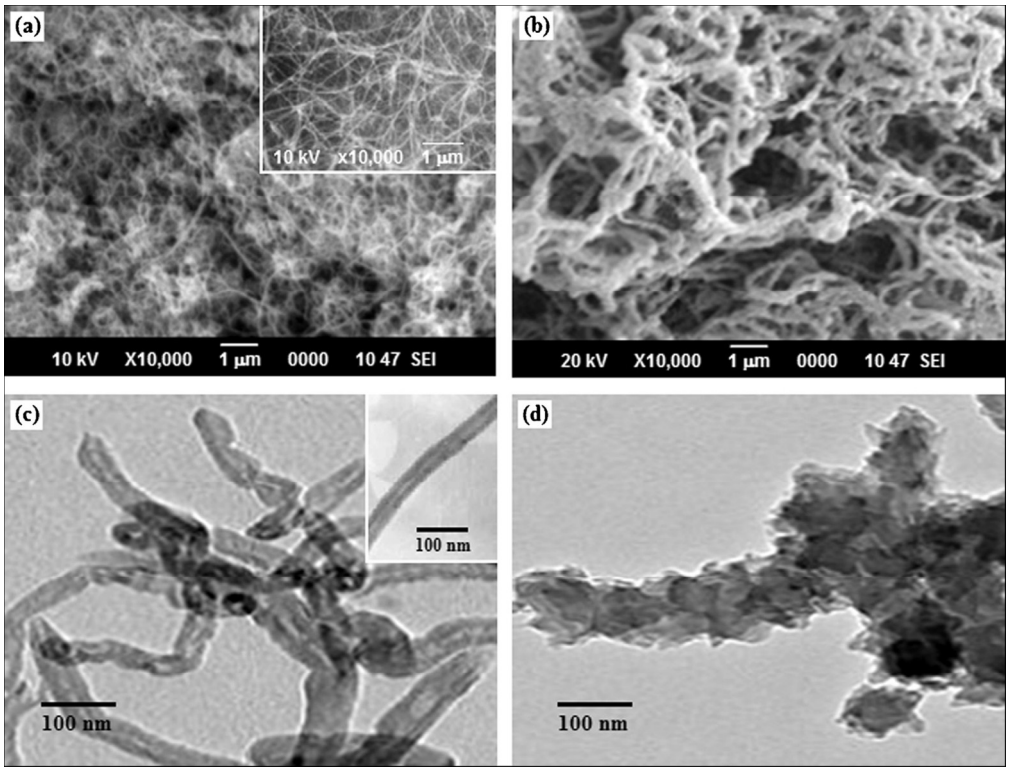

Figure 6. SEM (a) and (b) and dark field TEM (c) and (d) images of pristine MWCNT (inset), carboxyl-functionalized MWCNT and 2 wt% MWCNT-contained PANI/c MWCNT nanocomposite. (Reprinted with permission [68])
354x269mm (115 x 115 DPI)

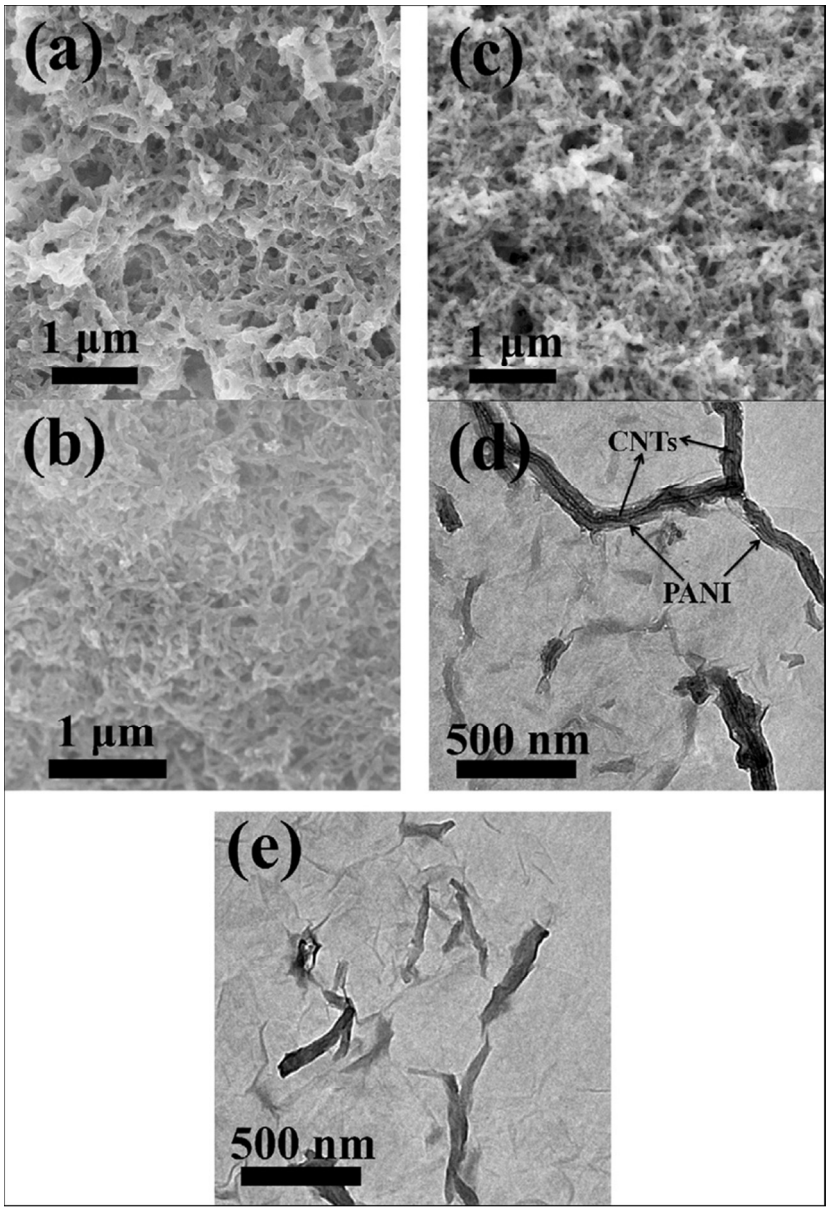

Figure 7. SEM images of PANI/CNT (a), PANI/CNT-2 (b) and PANI (c); TEM images of GO–PANI/CNT (d) and GO–PANI (e). (Reprinted with permission [90])

243x356mm (90 x 90 DPI)

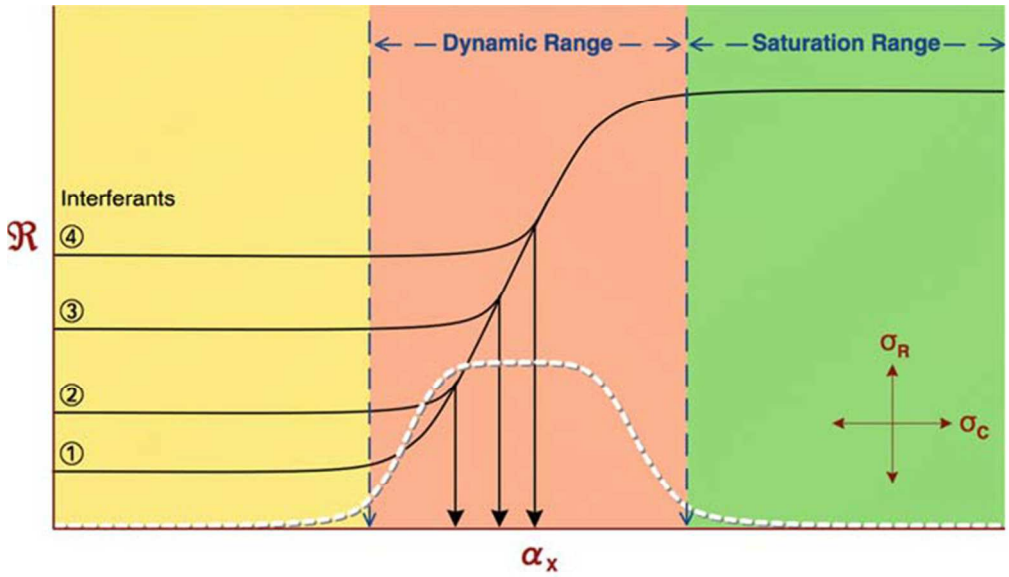

Figure 8. General response curve of a sensor [106]. (Reproduced from Principles of Chemical Sensors, 2009, page 4, Introduction to Sensors, Jiri Janata, with kind permission of Springer Science+Business Media.)
178x102mm (96 x 96 DPI)

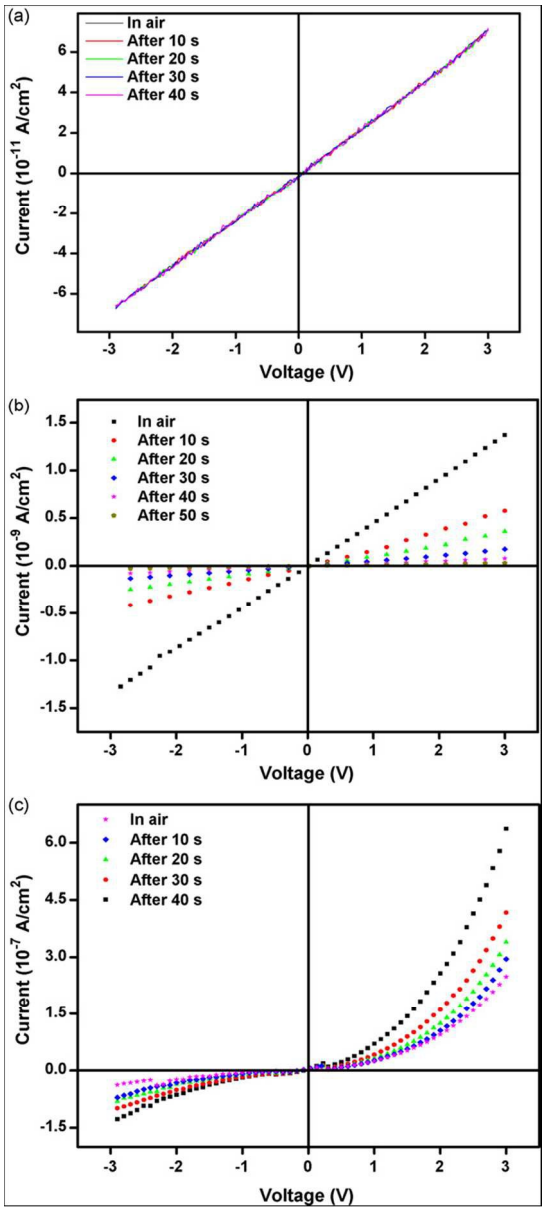

Figure 9. I–V curves (in the presence of ammonia gas) for (a) tin oxide, (b) polyaniline and (c) tin oxide/polyaniline nanocomposites. (Reprinted with permission [114])
175x391mm (96 x 96 DPI)

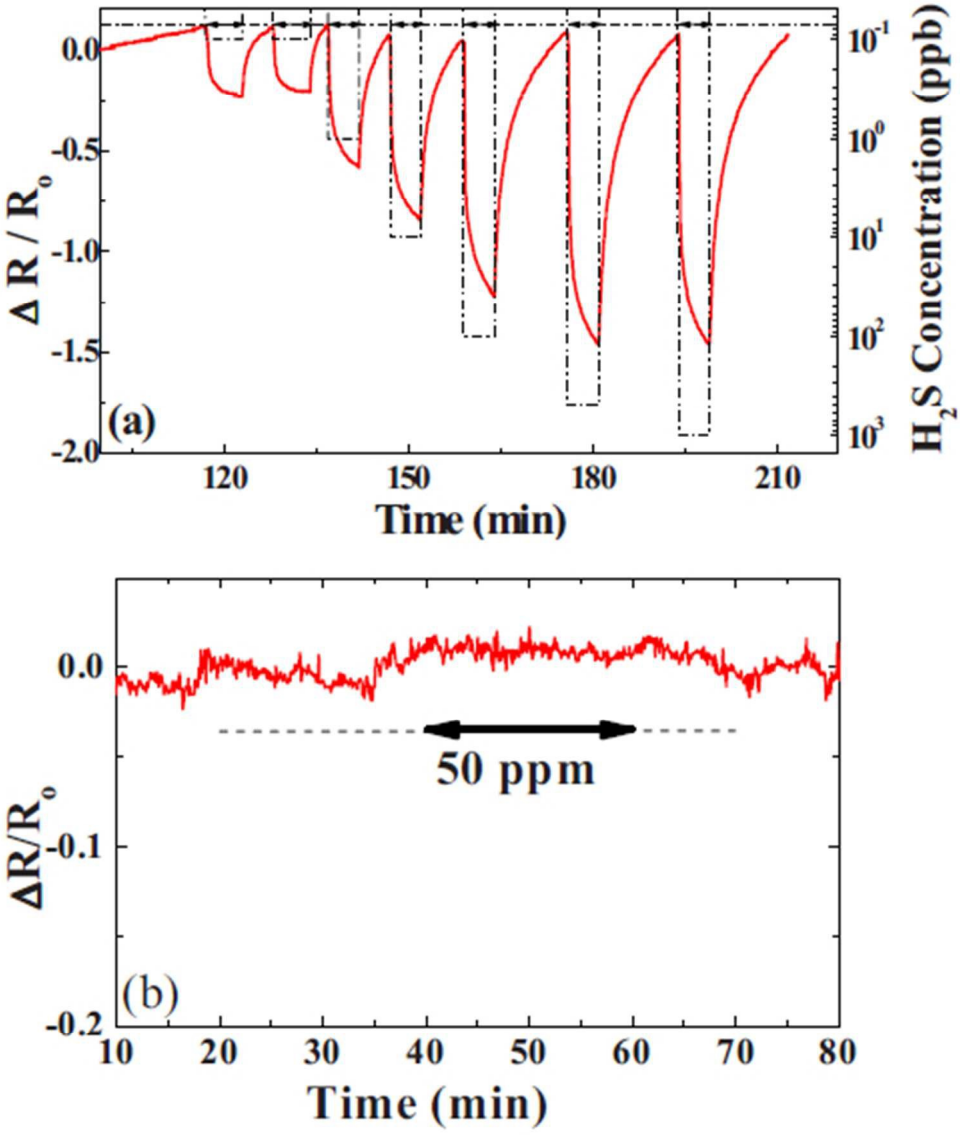

132x151mm (96 x 96 DPI)

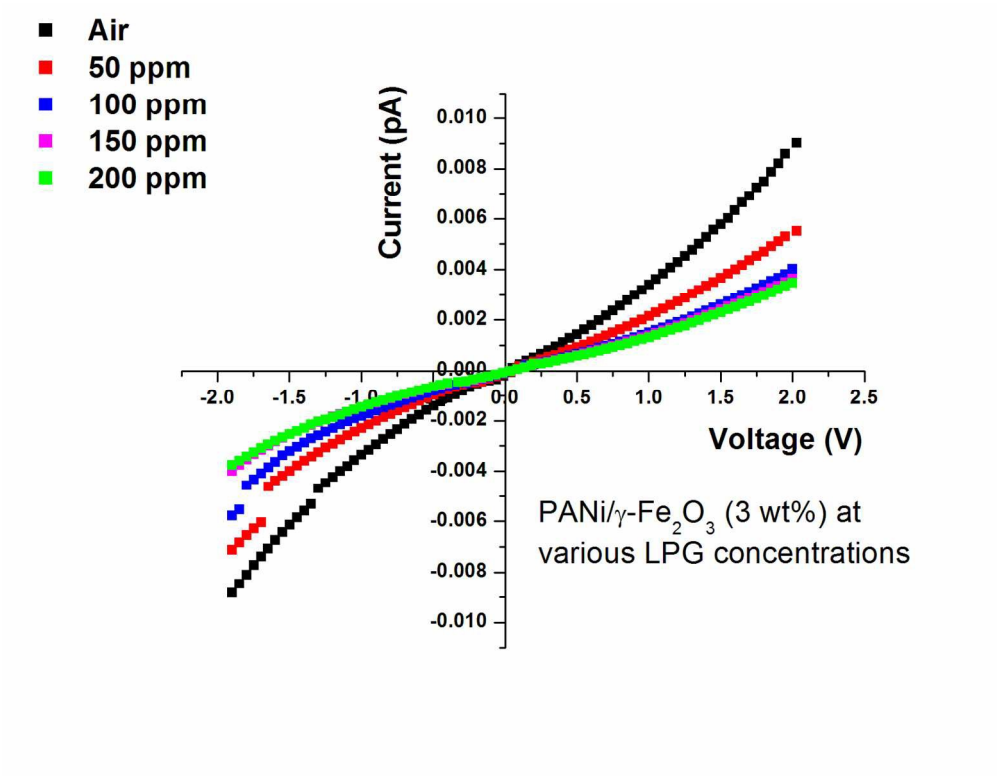

279x215mm (150 x 150 DPI)

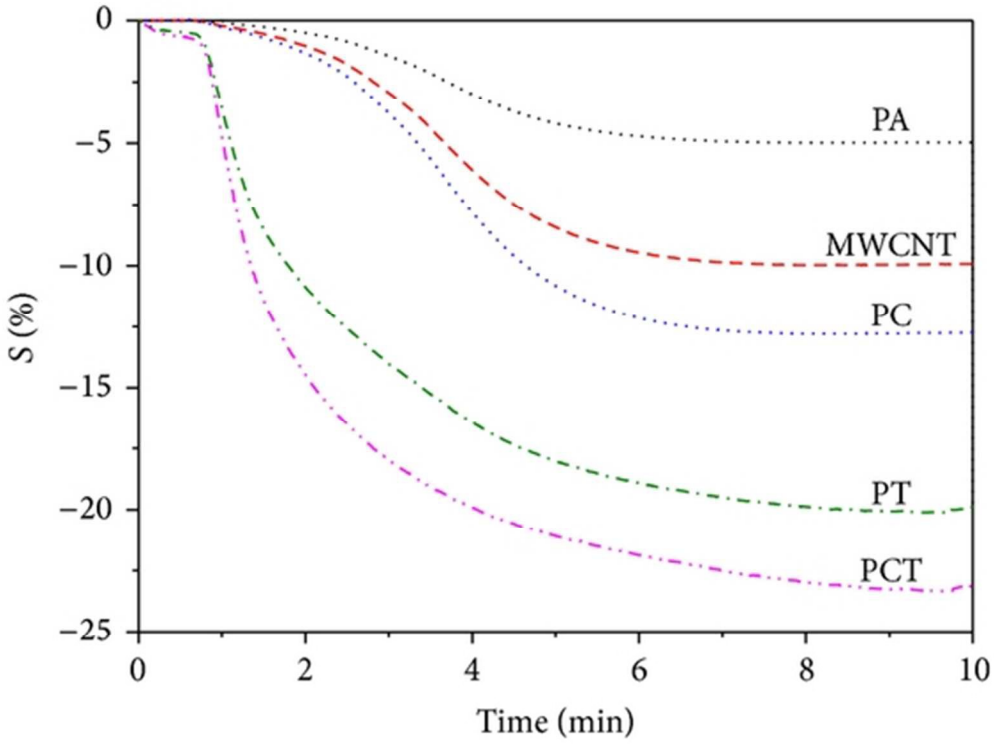

Figure 12. NO gas sensing behaviour of various samples under UV irradiation. (Reprinted with permission from [136])
150x112mm (96 x 96 DPI)

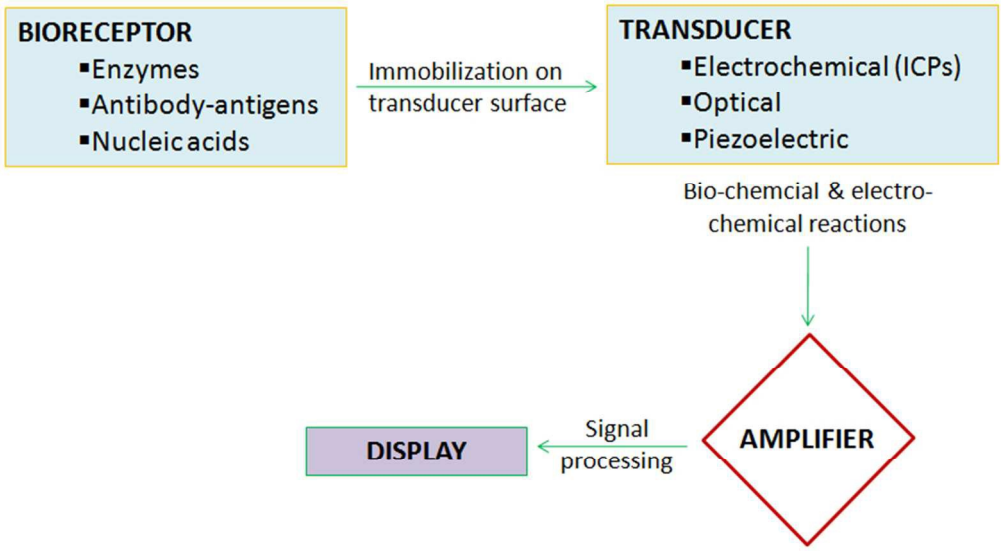

Figure 13. Schematic representation of biosensor operation.
211x116mm (96 x 96 DPI)

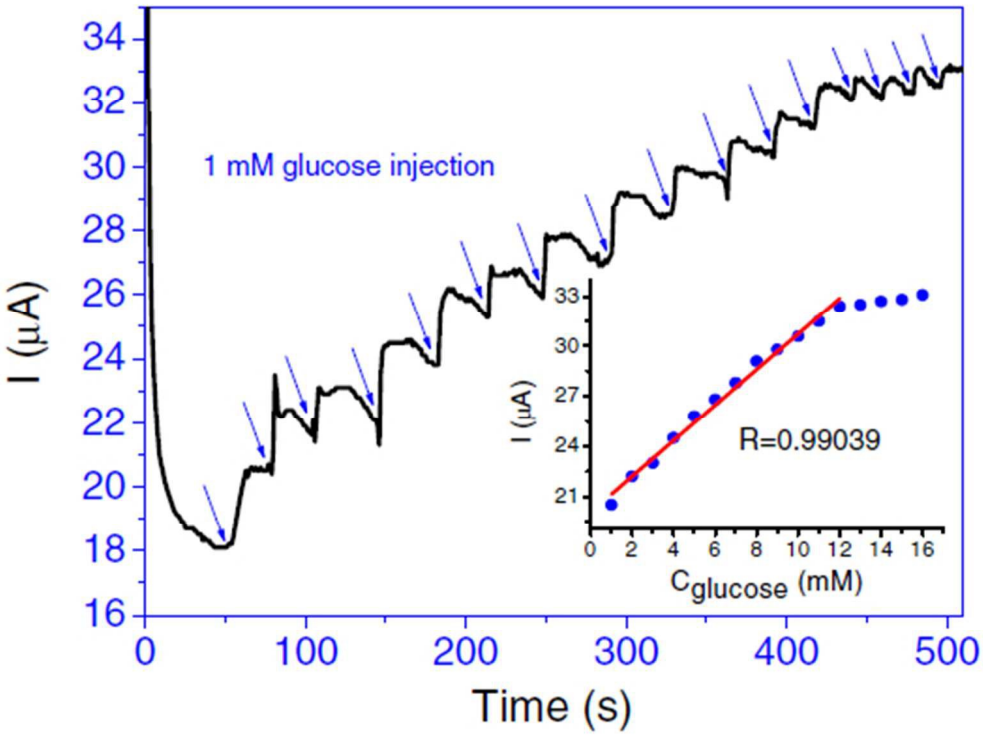

Figure 14. Amperometric response of GOx/PANi–MWCNT/IDμE upon increasing the glucose concentration in steps of 1mM at +0.6V (versus SCE) in PBS. Inset shows the calibration plot [156]. (Reproduced with permission from IOPscience)
141x104mm (96 x 96 DPI)

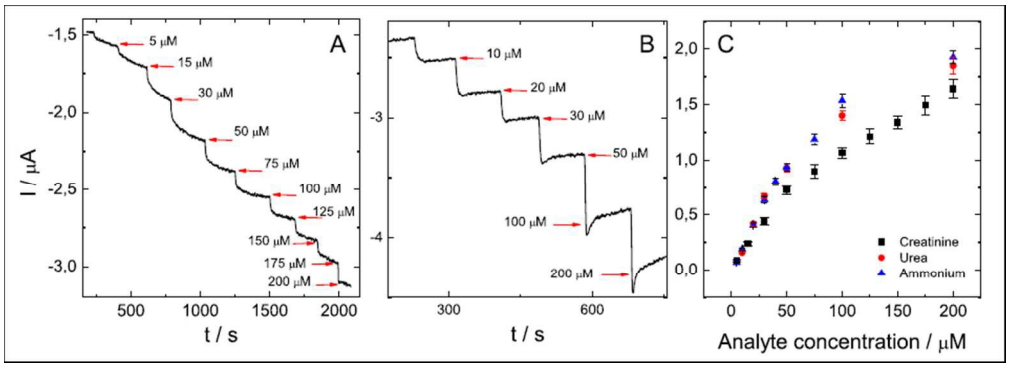

Figure 15. (A) An example of the amperometric response of the creatinine biosensor to successive additions of creatinine (-0.35 V, PBS pH 7.4). (B) An example of the amperometric response of the urea biosensor to successive additions of urea (-0.35 V, PBS pH 7.4). (C) Calibration curve for creatinine, urea and ammonium ion detection obtained at creatinine and urea biosensors and PANi-Nafion-Cu-modified SPE. (Reprinted with permission [175])
252x89mm (96 x 96 DPI)

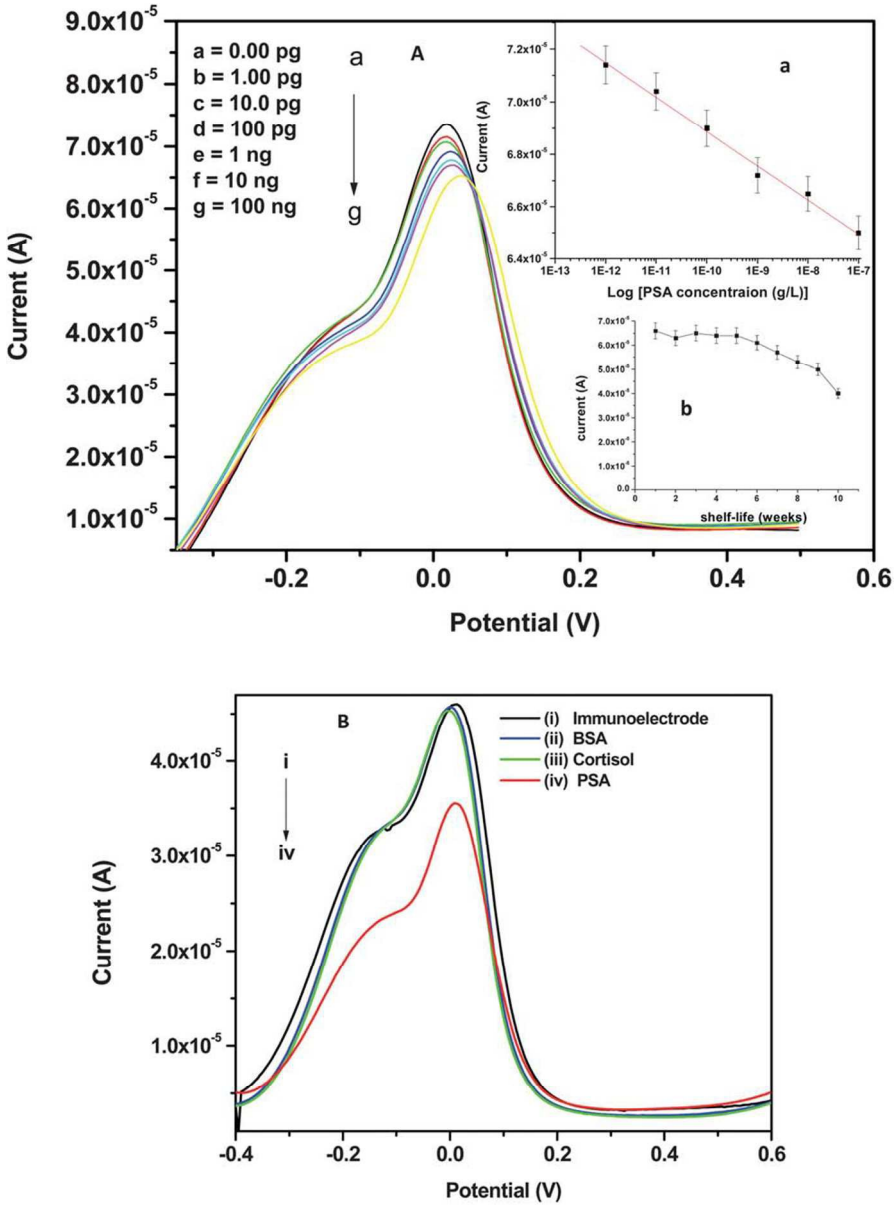

Figure 16. (A) Electrochemical response studies of the BSA/anti-PSA/ AuNP–PSA/Au immunoelectrode as a function of PSA (1 pg mL-1 to 100 ng mL-1) in PBS (10 mM, pH 7 containing 0.9% NaCl) using DPV technique. Inset (a) calibration curve between magnitude of electrochemical response current vs. logarithm of PSA concentration and inset (b) shelf-life studies of BSA/anti-PSA/AuNP–PSA/Au immunoelectrode. (B) Interference studies of BSA/anti-PSA/AuNP–PSA/Au immunoelectrode using BSA (10 ng mL-1) and cortisol (10 ng mL-1) with respect to PSA (10 ng mL-1). Reproduced from [178] with permission from The Royal Society of Chemistry.

259x351mm (96 x 96 DPI)

Table 1. Summary of synthesis methods for different types of PANI nanocomposites

Nanocomposite type	Secondary component	Synthesis method	References
PANI/Metal	Au	In situ interfacial polymerization involving one-step redox reaction	[35]
	Pt	In situ interfacial polymerization involving one-step redox reaction	[36], [38]
	Pt	Chemical and electrochemical synthesis by one-step redox reaction using K_2PtCl_6 as oxidant	[39]
	Ag	In situ chemical polymerization yielding core-shell morphology of PANI/Ag	[40]
	Ag	Ultrasound assisted miniemulsion method yielding Ag nanoparticles 5-10 nm in size	[41]
	Ag	Ultrasound-assisted reduction of Ag precursor followed by in situ polymerization of PANI in presence of nanosilver	[42]
	Ni	Aniline stabilized Ni particles prepared via ligand exchange reaction with aniline followed by polymerization	[43]
	Pd	Electroless surface deposition of Pd nanoparticles on electro-polymerized aniline on Ti electrode	[44]
	Pd	Sulphonated polystyrene nanofibers, used as template, coated over Pd nanoparticles followed by PANI coating and template removal	[45]
PANI/Metal oxide	Fe_3O_4	Micelle assisted method involving in situ nanoparticle formation	[46]
	TiO_2	Template synthesis	[48]
	γ-Fe_2O_3	In situ polymerization of aniline in presence of sonochemically prepared γ-Fe_2O_3 nanoparticles	[54]
	ZnO	Chemisorptions of PANI on the surface of hydrothermally grown ZnO	[47]

	ZnO	Physical mixture of PANI and ZnO nanoparticles	[58], [59]
	NiO	NiO nanoparticles embedded in PANI matrix via in situ polymerization	[52]
	Co_3O_4	In situ interfacial polymerization (in presence of Co_3O_4 nanoparticles)	[53]
	V_2O_5	V_2O_5 acts as template and oxidant for aniline polymerization yielding core-shell morphology	[55]
	V_2O_5	Hydrothermal synthesis of PANI-V_2O_5 nanosheets of thickness 10-20 nm via in situ intercalation polymerization	[56]
	RuO_2	Reduction of Ru(III) to Ru(II) forming ruthenium(II)-tetraaniline complex followed by composite formation by oxidation with H_2O_2	[57]
PANI/CNT or Graphene	CNT	Cable-like structure of PANI/CNT formed via *in situ* polymerization with CTAB functionalized CNT	[60]
	CNT	Electrospinning	[65]
	CNT	CNT functionalized by carboxylic acid followed by *in situ* polymerization	[68]
	Graphene	Amination of graphene sheet followed by covalent grafting with PANI	[69]
	Graphene	Polymerization of aniline on the surface of poly(styrenesulphonic acid) functionalized graphene with the sulphonic acid acts as dopant for PANI	[70]
	Graphene	Polymerization of anilinium dodecylsulphate (both a surfactant and a monomer) over graphene structure	[61]
	Graphene	Polymerization of aniline in presence of graphene oxide followed by its reduction to graphene	[73]
	Graphene oxide	Surfactant less method gives sandwich-like morphology	[71]

	Graphene oxide	In situ polymerization of aniline in presence of graphene oxide sheets yielded pH dependent morphologies	[72]
PANI/Chalcogenides	CdS	Polymerization of DBSA doped PANI followed by synthesis of CdS nanoparticles by co-precipitation	[74]
	CdS	In situ polymerization of aniline in presence of CdS prepared by sol-gel technique	[75]
	ZnS	Electrochemical polymerization of aniline in presence of ZnS nanoparticles	[76]
	CdSe	Ultrasound assisted inverse microemulsion method for nanocomposite preparation of PANI with CdSe quantum dots	[78]
PANI/Phthalocyanines or Porphyrins	Phthalocyanines	Electrostatic LBL technique forming multilayer composite	[79]
	Phthalocyanines	LBL films of PANI and Ni-tetrasulphonated phthalocyanins	[80]
	Porphyrins	J-aggregates assembled from Co-porphyrin acts as template for PANI electropolymerization giving rod-like morphology	[82]
PANI/Polymers	PVA	APS soaked PVA hydrogel immersed into aniline hydrochloride solution leads to formation of PANI in the bulk and on the surface of PVA	[83]
	PVA	PVA solution was spin coated on a FTO substrate followed by dip coating of PANI	[86]
	PVAc	Electrospinning	[88]
	PMMA	Solution casting of PANI nanofibers dispersed in PMMA/butanone solution	[87]
	PMMA	Electrospinning of mixture of CSA doped PANI and PMMA solutions	[89]
PANI/Multicomponent	CNT/graphene	In situ polymerized PANI/CNT dispersed in graphene oxide followed by its reduction to graphene	[90]

Graphene oxide/CNT	PANI formed by anodic elecptropolymerization on deposited on reduced graphene oxide/CNT papers	[93]
Fe_3O_4/CNT	Deposition of Fe_3O_4 on CNT followed by *in situ* polymerization of aniline	[94]
γ-Fe_2O_3/CNT	Coating of CNT and PANI/γ-Fe_2O_3 nanocomposite onto cotton thread	[95]
CNT/$CoFe_2O_4$	In situ chemical polymerization yielding reticular branched structure	[96]
Graphene oxide/CdSe	Graphene oxide/PANI composite formed by in situ polymerization followed by deposition of L-cysteine modified CdSe	[97]
SnO_2-ZnO	PANI coated solvothermally prepared SnO_2-ZnO nanoparticles coated over alumina	[98]
Pt-Pd	In situ polymerization of aniline in presence of PVP stabilized Pt-Pd colloids	[101]
Fe_3O_4-Au	In situ chemical polymerization in presence of mercaptocarboxylic acid which acts as template	[102]
PMMA/Ag	Electroless coating of Ag over PMMA capped PANI	[103]
PU-PMMA	PANI shell over a core of PMMA/PU	[104]
PU-PMMA	Interpenetrating network of PANI filled PU-PMMA	[105]

Table 2. PANI nanocomposite based gas sensors and biosensors

Sensor type	Analyte	Nanocomposite used	Salient features	References
Gas sensor	Methanol	PANI/Pd	Response to the order of ~ 10^4 for 2000 ppm methanol; Pd act as a catalyst for reduction of imine nitrogen in PANI by methanol	[108]
Gas sensor	Ethanol	PANI/Ag	Response > 2.0; Response time: 102-52 s for 2.5 mol% Ag	[109]
Gas sensor	Triethylamine, Toluene	PANI/Ag	Sensor response fitted with chemisorption and diffusion model	[110]
Gas sensor	Chloroform	PANI/Cu	Adsorption-desorption phenomenon at the surface of Cu clusters	[111]
Gas sensor	NH_3	PANI/TiO_2	High selectivity; response obtained by creation of depletion layer at the heterojunction of PANI and TiO_2	[112]
Gas sensor	NH_3	PANI/SnO_2	Neat PANI shows reduced behaviour while nanocomposite shows an oxidized behaviour in gas environment	[114]
Gas sensor	NH_3	PANI/SnO_2	CSA doping increase response from 72% to 91% at 46 s response time	[115]
Gas sensor	NH_3	PANI/PMMA	Trace level detection (1 ppm) due to PANI coated highly aligned PMMA microfibers	[116]
Gas sensor	NH_3	PANI/sulphonated Ni phthalocyanine	Ni phthalocyanine catalyzed electrodeposition of PANI influence sensor response	[117]
Gas sensor	H_2S	PANI/$CuCl_2$	Trace level H_2S detection; H2S exerted oxidizing effect on PANI due to preferential binding of $CuCl_2$ with S^{2-} ion with evolution of HCl	[118]
Gas sensor	H_2S	PANI-CdS	Response of ~ 48% for 100 ppm H_2S	[120]
Gas sensor	H_2S	PANI/Au	Trace level H_2S detection (0.1 ppb); formation of H^+ ions protonates PANI	[121]

Gas sensor	LPG	CdSe/PANI	Response ~ 70% for 0.08 vol% LPG	[122]
Gas sensor	LPG	PANI/γ-Fe_2O_3	Response: 1.3 for 200 ppm LPG	[54]
Gas sensor	LPG	PANI/TiO_2	Response ~ 63% for 0.1 vol% LPG	[123]
Gas sensor	LPG	PANI/CdSe	Response ~ 80% for 1040 ppm LPG	[124]
Gas sensor	LPG	PANI/ZnO	Response ~ 81% for 1040 ppm LPG	[125]
Gas sensor	Water vapour	PANI/Co	Response time: 8 s, recovery time: 1 min; water vapour adsorption modifies electrical conductivity	[127]
Gas sensor	Water vapour	PANI/Ag	Sensor's sensitivity influenced by critical quantum confinement of Ag nanoparticles	[128]
Gas sensor	Water vapour	PANI/Ag-V_2O_5	Increase in conductivity with increasing humidity due to influence of humidity on macromolecular arrangement	[131]
Gas sensor	CH_4	PANI/In_2O_3	Temperature dependant response to CH_4	[133]
Gas sensor	CO	PANI/SnO_2	Trace level detection of CO (1 ppm)	[134]
Gas sensor	CO	PANI/SWCNT	Highly selective towards CO in a gas mixture	[135]
Gas sensor	NO	PANI/TiO_2/ MWCNT	Detection occurs through decomposition of NO into HNO_2, NO_2 and HNO_3 under UV irradiation	[136]
Gas sensor	NO_2	SnO_2-ZnO/PANI	Temperature dependent response ~ 368 at 35 ppm NO_2 at 180 °C	[137]
Gas sensor	H_2	PANI/WO_3	Detection through formation of tungsten–dihydrogen complexes	[140]
Gas sensor	H_2	PANI/PtO_2	Catalytic oxidation of H_2 gas to water decreasing resistance of PANI	[141]
Gas sensor	CO_2	PANI/ chloroaluminium phthalocyanine	Sensitivity range of 0.05–7.20	[142]

Biosensor	Glucose	Au/PANI	Sensitivity: 2.3 mA/M Detection limit: 5.0×10^{-7} mol/L	[152]
Biosensor	Glucose	Graphene/PANI/ Au	Reagentless amperometric glucose biosensor Detection limit: 0.6 mM	[153]
Biosensor	Glucose	PANI-TiO_2	Sensitivity: 11.4 μA mM^{-1} Detection limit: 0.5 μM	[157]
Biosensor	Cholesterol	PANI/Au/chitosan	Sensitivity: 34.77 μA $mM^{-1}cm^{-2}$ Detection limit: 1 μM	[160]
Biosensor	Cholesterol	PANI/MWCNT	Sensitivity: 6800 nA mM^{-1} Detection range: 1.29-12.93 mM	[162]
Biosensor	Cholesterol	PANI/CMC	Sensitivity: 0.14 mA/mM cm^2 Detection limit: 1.31 mM	[163]
Biosensor	Cholesterol	PANI/Au/ Graphene	Coupled enzyme reactions Sensitivity: 0.42 μAmM^{-1}	[164]
Biosensor	H_2O_2	PANI/Polyester sulphonic acid	Sensitivity: 1.33 μA μM^{-1} Detection limit: 0.185 μM	[169]
Biosensor	H_2O_2	PANI/Chitosan	Linear response range: 1×10^{-5} - 1.5×10^{-3}M Detection limit: 5×10^{-7}M	[170]
Biosensor	Uric acid	Fe_3O_4/Chitosan/ PANI	Sensitivity: 0.44 mA mM^{-1} Detection limit: 0.1 μM	[171]
Biosensor	Creatinine	PANI/cMWCNTs	Tri-enzyme system with creatinine amidohydrolase, creatine amidinohydrolase and sarcosine oxidase Sensitivity: 40 μA/mM/cm^2 Detection limit: 0.1 μM	[173]
Biosensor	Creatinine, Urea	Cu/PANI	Ammonium ion-specific biosensor; Sensitivity: 95 mA M^{-1} cm^{-2} (creatinine) and 91 mA M^{-1} cm^{-2} (urea)	[175]
Biosensor	Salbutamol	Au nanoparticles, Prussian blue, poly(acrylic acid) and Au-graphene	Linear response range: 0.08 – 1000 ng/mL Detection limit: 0.04 ng/mL	[176]
Biosensor	Interleukin-6	GO/PANI/CdSe	Linear response range: 0.0005 – 10 ng/mL Detection limit: 0.17 pg/mL	[177]
Biosensor	Prostate-specific antigen	PANI/Au	Sensitivity: 1.4 μA M^{-1} Detection limit: 0.6 pg mL^{-1}	[178]

Biosensor	Chlorpyrifos	Au/PANI/ cMWCNTs/chitosan	Linear response range: 0.1 – 40×10^{-6} mg/ml and 40×10^{-6} – 500×10^{-6} mg/ml Detection limit: 0.06×10^{-6} mg/ml	[179]
Biosensor	Estradiol	Graphene/PANI	Linear response range: 0.04 – 7.00 ng/mL Detection limit: 0.02 ng/mL	[180]
Biosensor	Benzo[a]pyrene	Fe_3O_4/PANI/Nafion	Linear response range: 8 pM – 2 nM Detection limit: 4 pM	[181]
Biosensor	LDL	Au-AgCl/PANI	Label-free biosensor Detection limit: 0.34 pg/mL	[182]
Biosensor	DNA hybridization	PANI/GO	Linear response range: 275 to 551 g/mL (ssDNA immobilized electrode) Detection limit: 29.34 g/mL	[183]
Biosensor	BCR/ABL fusion gene (in chronic myelogenous leukemia)	Au/PANI on GCE	Detection limit: 2.11 pM	[186]
Biosensor	DNA hybridization	PPY/PANI/Au	Label-free DNA biosensor Detection limit: 10^{-13} M	[187]
Biosensor	Phosphinothricin acetyltransferase gene	PANI/MWCNT	Linear response range: 1.0×10^{-13} - 1.0×10^{-7} mol/L Detection limit: 2.7×10^{-14} mol/L	[190]
Biosensor	DNA bases	PANI/ cMWCNTs	Sensitivity: 1.6, 1.9, 1.5 and 2.4 $\mu A/cm^2$ μM Detection limit: 4.8, 2.9, 1.3 and 1.3 μM (for guanine, adenine, thymine, and cytosine, respectively)	[192]

Synthesis and Sensing Applications of Polyaniline Nanocomposites: A Review

Tanushree Sen[1], Satyendra Mishra[1]and Navinchandra G. Shimpi[2]*

[1]*University Institute of Chemical Technology, North Maharashtra University, Jalgaon - 425001, Maharashtra, India.*

[2]*Department of Chemistry, University of Mumbai, Vidyanagri, Santa Cruz (E) 400 098 Maharashtra, India*

Graphical Abstract